UNIVERSITÄT ZU LÜBECK

From the Institute of Experimental and Clinical

Pharmacology and Toxicology

of the University of Lübeck

Director: Prof. Dr. Markus Schwaninger

Mechanisms of ischemic brain damage in hyperglycemic strokes

Dissertation

in Fulfillment of Requirements

for the Doctoral Degree

- Dr. rer. nat.-

of the University of Lübeck

Submitted by

Mahtab Ahmad Khan

from Multan, Pakistan

Lübeck, 2015

First referee: Prof. Dr. Markus Schwaninger

Second referee: Prof. Dr. Tamás Laskay

Chairman: Prof. Dr. Wolfgang Jelkmann

Date of oral examination: 20/08/2015

Approved for printing: 24/08/2015

ACKNOWLEDGEMENT

I would like to acknowledge all the people who have supported me during these years of work. Unfortunately, I cannot mention all of them; nevertheless, I assure them all of my sincerest thanks.

First of all, I would like to express my immense gratitude to my supervisor Prof. Markus Schwaninger, for providing me the opportunity to work in his group and for guiding me through these years. His constructive criticism, great support and optimism towards my work have motivated me at every stage of this thesis.

I am very grateful to Dr. Mahbubur Rahaman for all the great support in teaching me the MCAO technique. I would like to thank my post-doc colleagues, Dr. Jan Wenzel and Dr. Helge Müller-Fielitz for teaching me all I had to know about fluorescence and confocal microscopy, Dr. Jochen Ohnmacht and Dr. Godwin Dogbevia for their help in understanding the imaging software. I would also like to thank Dr. Dirk A Ridder for his advice in statistics and his ever supportive attitude. I would like to thank Mr. Dr. Walter Häuser for providing his expertise and support in maintaining the mouse lines for the whole experiments. I would like to thank Dr. Thomas Flemming from the University of Heidelberg for kindly providing the $RAGE^{-/-}$ mice. I am grateful to all the members from our animal core facility that contributed in any way to my work and supported me during these years. I would like to thank Mr. Sajad Ahmad for his guideline in MS office. I appreciate the efforts of Mr. Julian Assmann for translating the summary of my project. I am grateful to Ms. Sina Schultz for her extensive contribution to the study.

I am thankful to Higher Education Commission (HEC) Pakistan for granting me a scholarship to pursue my PhD and Deutscher Akademischer Austausch Dienst (DAAD) for their wonderful coordination in Germany.

I am really thankful to my family and my parents for being there for me in every conceivable way and a special thanks to my father, for his encouragement and support.

Mahtab Ahmad Khan

ZUSAMMENFASSUNG

Es ist bekannt, dass eine Hyperglykämie die Folgen eines Schlaganfalles verschlimmert. Eine Hyperglykämie ist beim akuten Schlaganfall sehr häufig, unabhängig von einer vorbestehenden Diabeteserkrankung.

In dieser Arbeit wurden die möglichen Mechanismen untersucht, die zu einem schwereren Verlauf von Schlaganfällen unter hyperglykämischen Bedingungen führen.

Dazu wurde bei Mäusen die A. cerebri media verschlossen (*middle cerebral artery occlusion,* MCAO), um einen Schlaganfall herbeizuführen. Die Glukosekonzentration im Blut wurde durch intraperitoneale Glukoseinjektionen erhöht. Anschließend wurde das Infarktvolumen ermittelt. Mittels Durchflusszytometrie wurden die inflammatorischen Zellpopulationen in Gehirn und Blut bestimmt. Zusätzlich wurden die *in vivo* Daten mit Immunfluoreszenzfärbungen und Konfokalmikroskopie bestätigt.

Durch die Verwendung von chimären Mäusen konnten wir zeigen, dass aus dem Knochenmark stammende Monozyten /Makrophagen schon 24 Stunden nach dem Schlaganfall in das Gehirn einwandern und sich deren Zahl nach 48 Stunden weiter erhöht hat. Außerdem haben wir beobachtet, dass Nikotinsäure und ß-Hydroxybutyrat (BHB) ihren neuroprotektiven Effekt über den Hydroxycarboxylsäurerezeptor 2 (*hydroxy-carboxylic acid receptor 2,* HCA_2 / GPR109a*)* vermitteln. Dieser Rezeptor befindet sich auf den alternativ aktivierten Monozyten / Makrophagen, den sogenannten M2-Makrophagen.

Das Infarktvolumen unter hyperglykämischen Bedingungen war 48 Stunden nach MCAO signifikant erhöht. Mittels Durchflusszytometrie konnte gezeigt werden, dass M2-Makrophagen ($CD45^{Hi}$ $CD11b^{+}$ $Ly6\text{-}G^{-}$ $Ly6\text{-}C^{Lo}$), die einen protektiven Effekt vermitteln, unter diesen

Bedingungen erniedrigt sind. Für eine nähere Untersuchung der Rolle dieser Zellen haben wir von Monozyten abstammende Zellen in CD11b-DTR Mäusen deletiert. Um den Erfolg dieser Methode zu zeigen, wurde mit Hilfe von Durchflusszytometrie das Blut von Wildtyp- und CD11b-DTR Mäusen analysiert. Die Auswertung zeigte, dass der Anteil an $CD11b^{+}$ Zellen um 80-85% reduziert war, ohne die Anzahl an neutrophilen Granulozyten zu beeinflussen.

Nach Deletion der von Monozyten abstammenden Zellen war Infarkt unter hyperglykämischen Bedingungen nicht vergrößert , während dies für Wildtyp-Mäuse der Fall war.

Die Bildung von "*advanced glycation end products" (*AGEs) und ihre Interaktion mit dem Rezeptor für AGEs (RAGE) vermitteln den schädlichen Effekt von hyperglykämischen Schlaganfällen. Für die Analyse des RAGE-assoziierten Gehirnschadens wurde eine MCAO in $RAGE^{-/-}$ Mäusen durchgeführt. Im Vergleich zu hyperglykämischen Kontrollen wiesen Mäuse, die defizient für RAGE waren, ein signifikant verringertes Infarktvolumen auf.

Arginase I (ArgI) ist ein spezifischer Marker für M2-Makrophagen. Die Quantifizierung der ArgI-exprimierenden Makrophagen mittels Immunfluoreszenzfärbung und Konfokalmikroskopie ergab eine Reduktion unter hyperglykämischen Bedingungen.

Die oben aufgeführten Daten zeigen, dass eine Reduktion der protektiven Makrophagen im Gehirn unter hyperglykämischen Bedingungen zu einem vergrößerten Infarktvolumen führt.

SUMMARY

It is well established that hyperglycemia aggravates stroke outcome. Hyperglycemic conditions are likely to be present in stroke patients regardless of pre-existing diabetes.

In this study, I have investigated the possible mechanisms involved in worsening of stroke outcomes under hyperglycemic conditions. I occluded the middle cerebral artery (MCA) to produce stroke in mice. To elevate the glucose concentration in blood, I have injected glucose intraperitoneally. Then, the infarct volume was measured. I used flow cytometry to identify the inflammatory cell population in brain and blood. Finally, immune fluorescence and confocal microscopy have been utilized to confirm the in vivo data.

By using chimeric mice strong evidence was obtained that bone marrow-derived monocytes and / or macrophages migrate to the brain after stroke as earlier as 24 hours and their number increased after 48 hours. In previous experiments we had observed that nicotinic acid and ß-hydroxyl butyrate (BHB) mediate their neuroprotective action through hydroxy-carboxylic acid receptor 2 (HCA_2, GPR109A). This receptor is located on the alternatively activated monocytes and/or macrophages. These cells are also called M2 macrophages.

The infarct volume is significantly increased under hyperglycemic conditions after 48 hours of MCAO. Using flow cytometry, I confirmed that M2 macrophages ($CD45^{Hi}$ $CD11b^{+}$ Ly6-G^{-} Ly6-C^{Lo}), that are protective in action, are decreased under hyperglycemic conditions. To investigate their role further, I ablated monocyte-derived cells in CD11b-DTR mice. To confirm the ablation, I performed flow cytometry of blood cells after diphtheria toxin treatment in wild-type and CD11b-DTR mice. These experiments showed that 80-85% of $CD11b^{+}$ cells were depleted in CD11b-DTR mice without affecting neutrophils. The infarct volume in CD11b-DTR mice did not differ under normoglycemic and hyperglycemic conditions while the infarct volume

remained higher in wild-type hyperglycemic mice. Advanced glycation end products (AGEs) formation and their interaction with the receptor for AGEs (RAGE), mediate the deleterious effect of hyperglycemic stroke. To investigate the role of RAGE associated brain damage, I performed MCAO in $RAGE^{-/-}$ mice. Mice lacking RAGE showed significantly reduced infarct volumes as compared to hyperglycemic controls. Arginase I (ArgI) is a specific marker for M2 macrophages. Using immunofluorescence and confocal microscopy the number of ArgI expressing macrophages were decreased under hyperglycemic condition.

In view of above experiments, it is concluded that a reduced number of protective macrophages leads to larger infarct volumes under hyperglycemic conditions.

Affectionately dedicated to my respected teachers and my beloved parents

CONTENTS

LIST OF FIGURES

ABBREVIATIONS

AGE	Advanced glycation end products
ANOVA	Analysis of variance
Arg I	Arginase I
ATP	Adenosine tri-phosphate
BAC	Bacterial artificial chromosome
BHB	Beta hydroxyl butyrate
BM	Bone marrow
BSA	Bovine serum albumin
CCA	Common carotid artery
CD11b	Cluster of differentiation molecule 11B
DABCO	1, 4-diazobicyclo [2.2. 2] octane
dpi	Dots per inches
DT	Diphtheria toxin
FACS	Fluorescence activated cell sorting
GPCR	G-protein coupled receptor
HCA_2	Hydroxy carboxylic acid receptor 2
HG	Hyperglycemic

ICA	Internal carotid artery
ip	Intraperitoneal
Ly-6C	Lymphocyte antigen 6 complex
MCAO	Middle cerebral artery occlusion
MG	Methylglyoxal
NG	Normoglycemic
RAGE	Receptor for advanced glycation end products
Rcf	Relative centrifugal force
TBE	Tribomoethanol
TIF	Tagged image file
WHO	World health organization
WT	Wild-type

1. INTRODUCTION

The world health organization (WHO) fact sheet had reported that 15 million people suffer from stroke every year. Out of those 5 million people had died and another 5 million people were permanently disabled (Anonymous 2008). A large number of other clinical data also reported the association of hyperglycemia with poor stroke outcome (Moulin, Tatu et al. 1997; Weir, Murray et al. 1997). Therefore, hyperglycemia (plasma glucose concentration > 8 mmol/l) is regarded as an independent risk factor in worsening of stroke (Counsell, McDowall et al. 1997).

1.1. Stroke

Stroke is caused by reduced blood flow by successful restoration of the blood supply the ischemic region can be protected against permanent damage. Experimental data have shown that parts of the ischemic zone can be saved. This area is called penumbra. In the penumbra, the blood flow is indeed so low that the function cannot be maintained but still the blood flow is sufficient to ensure the structural metabolism of the tissue. Under favorable conditions, the penumbra can survive but under unfavorable conditions it is also infarcted (Figure 1). Hours after the event different pathological mechanisms endanger the survival of the penumbra (Dirnagl, Iadecola et al. 1999).

Figure 1 ***Schematic diagram of ischemic stroke.***

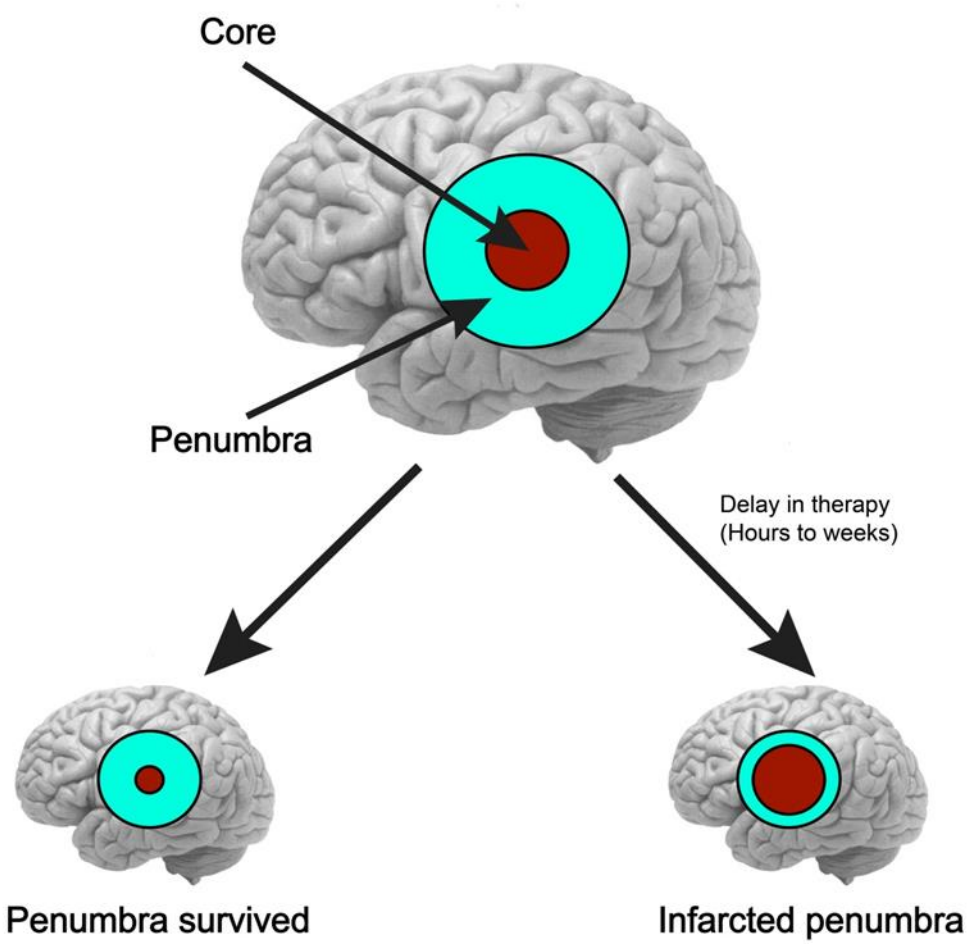

1.2. Animal stroke models

Different animal species have been used in stroke study and this has enhanced the understanding of stroke pathophysiology. Mice and rats are widely used animals in stroke studies (Casals, Pieri et al. 2011). The selection of a suitable animal model is very important while interpreting the results and inferences. Numerous techniques have been used to induce an ischemic stroke; for example complete and incomplete ischemia, focal and multifocal cerebral ischemia (Watson, Dietrich et al. 1985; Dietrich, Ginsberg et al. 1986; Ahmad, Saleem et al. 2010; Mecca, Regenhardt et al. 2011; Beretta, Riva et al. 2013; Speetzen, Endres et al. 2013; Shmonin, Melnikova et al. 2014). Among these stroke models, transient and permanent vessel occlusion are two commonly employed types of focal cerebral ischemia. In the transient stroke model, a silicon-coated filament is inserted in an internal carotid artery (ICA) through the common carotid artery (Ahmad, Saleem et al. 2006). The duration of the filament placement (occlusion) inside the ICA and its removal (reperfusion) differ in different studies. In the permanent stroke model, which is more reproducible and reliable, the middle cerebral artery (MCA) is blocked permanently (occlusion) either by ligation (Davis, Lay et al. 2013) or by electrical coagulation (Rahman, Muhammad et al. 2014).

In this study, we used a permanent stroke model in mice, which involves craniotomy and occlusion of the distal MCA.

Figure 2 ***Methodology based classification of the ischemic stroke.***

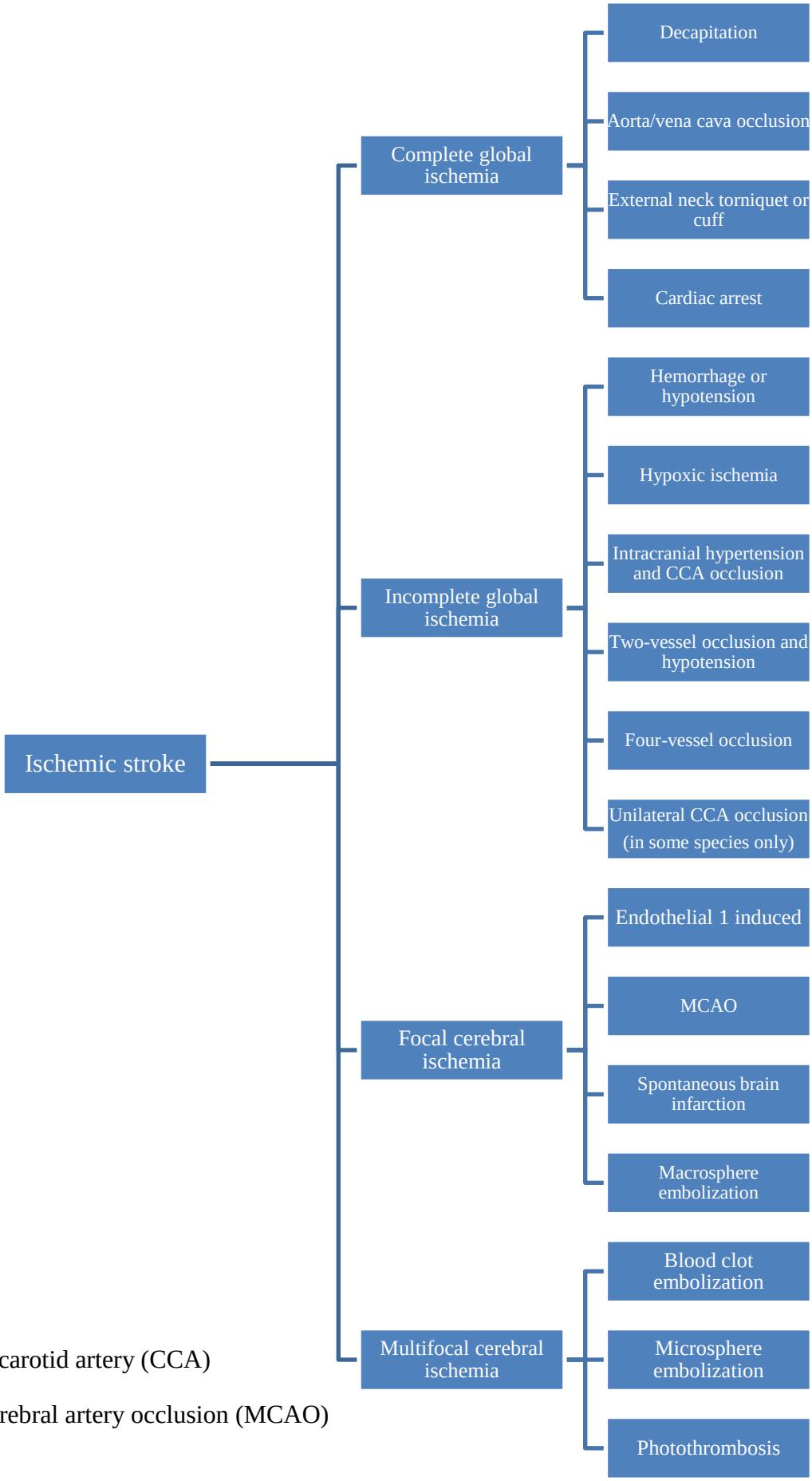

Common carotid artery (CCA)

Middle cerebral artery occlusion (MCAO)

1.3. Hyperglycemia worsens the stroke outcome

Hyperglycemia is likely to be present in stroke patients with or without preexisting diabetes, especially in patients not older than 65 years of age (Allport, Butcher et al. 2004; Kissela, Khoury et al. 2005; Kruyt, Biessels et al. 2010). It has also been reported that hyperglycemia increases the risk of stroke by about 1.7- to 2.1-times (Spencer, Pirie et al. 2008). Hyperglycemia has also been found to be involved in increasing the infarct size and mortality in animal stroke models (Anderson, Tan et al. 1999; Garg, Chaudhuri et al. 2006). Ischemic stroke is accompanied by a global stress response that involves the activation of hypothalamic-pituitary-adrenal (HPA) axis and hyperglycemia (Kruyt, Biessels et al. 2010).

Figure 3 ***Mechanism of hyperglycemia in ischemic stroke patients***

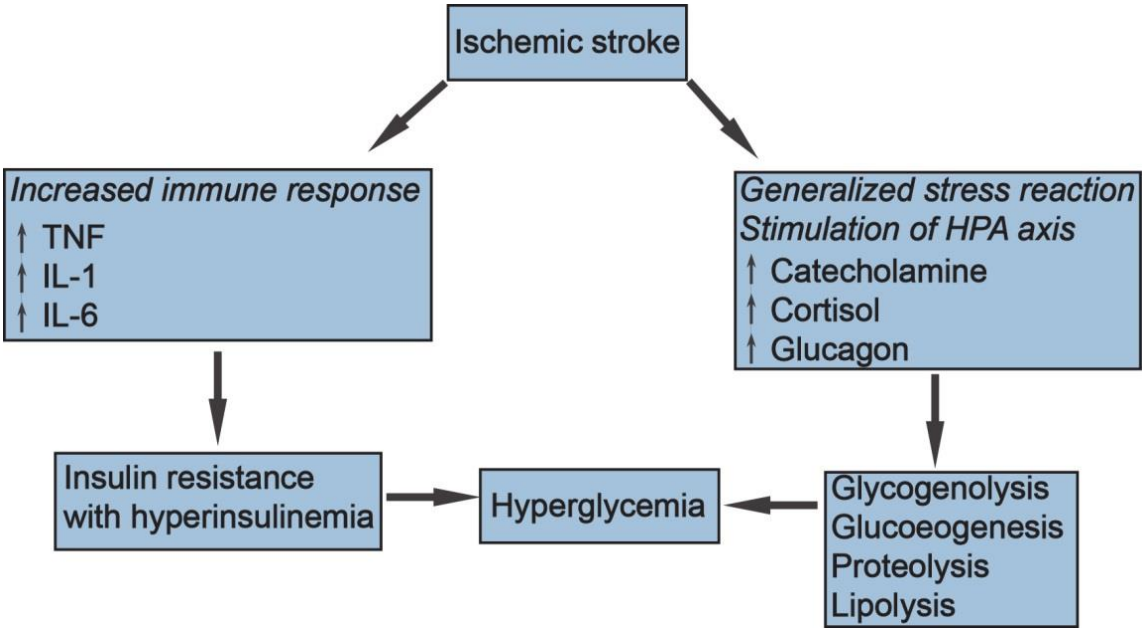

Stress reaction itself contributes to hyperglycemia after ischemic stroke. Figure modified from Kruyt, Biessels et al. 2010 (Kruyt, Biessels et al. 2010). Hypothalamic-pituitary-adrenal (HPA) axis, Tumor necrosis factor (TNF), Interleukin-1 (IL-1), Interleukin-6 (IL-6).

1.4. Glucose metabolism and advanced glycation end (AGE) products

Glucose is a substantial source of nutrient for brain except during prolonged starvation. Glycolysis is the major pathway of glucose metabolism and it occurs in the cytosol of all cells. This process can occur either aerobically or anaerobically (Robert K. Murray 2003). During ischemic conditions (e.g., ischemic stroke), there is a reduced oxygen and glucose supply to the ischemic region that will result in cell death (Robbins and Swanson 2014). Other tissues, including heart, can utilize amino acids and fatty acids, but the entry of most of these nutrients to the brain is difficult due to the blood-brain barrier (Siesjo 1978). Glucose metabolism is disturbed in the majority of acute stroke patients (Matz, Keresztes et al. 2006). The rate of glycolysis increases 4- to 7-fold after brain ischemia, as observed in different experimental mouse models. Anaerobic glycolysis will synthesize less (2 moles) ATP (adenosine tri-phosphate) molecules per mole of glucose oxidized than aerobic metabolism. For this reason, the glucose demand increases under anaerobic conditions as compared to aerobic conditions (Robert K. Murray 2003).

Advanced glycation end (AGE) products are proteins or lipids that have reacted non-enzymatically with sugar (Vlassara, Brownlee et al. 1981; Goldin, Beckman et al. 2006). The degree of hyperglycemia, the extent of oxidative stress and rate of turnover of proteins are vital factors for the synthesis of AGEs. During the formation of AGEs, either glucose or dicarbonyl compounds react with proteins at lysine and arginine residues by means of the Maillard reaction (Thornalley 2005). The accumulation and interaction of AGEs with receptor for advanced glycation end products (RAGE) produce permanent damage to the tissue; stimulate cytokines and reactive oxygen species (ROS) production as well as the modification of intracellular

proteins (Brownlee 1995; Srikanth, Maczurek et al. 2011). However, the role of RAGE in hyperglycemic stroke has not been studied.

Figure 4 Formation of AGE

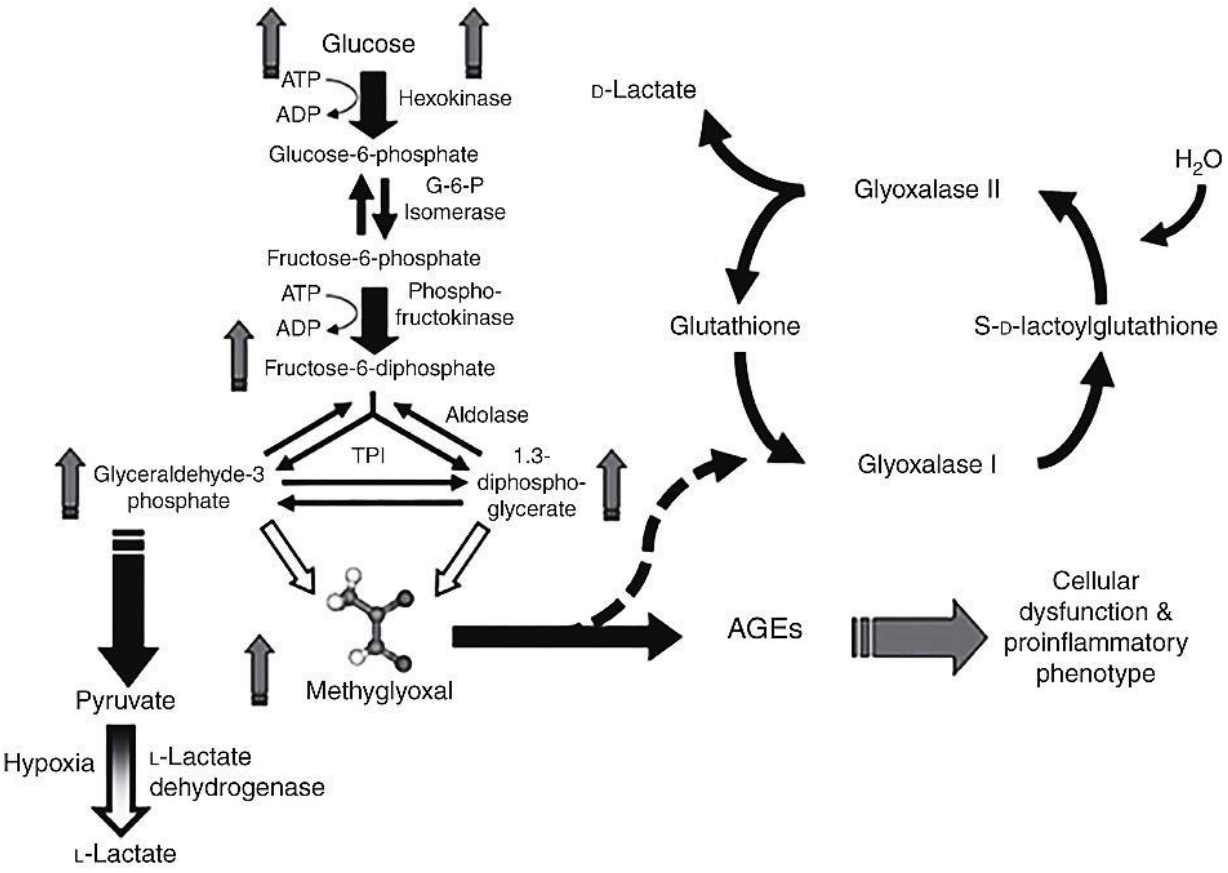

Glucose metabolism via the glycolysis is shown on the left. Intracellular methylglyoxal (MG) formation and its elimination. Adopted from Kiefer, Fleming et al. 2014 (Kiefer, Fleming et al. 2014). The breakdown of glucose to pyruvate via the Embden–Meyerhof pathway of glycolysis is shown on the left. The spontaneous dephosphorylation of triose phosphate intermediates (TPI) leads to the formation of methylglyoxal (MG). MG either synthesizes advanced glycation end products or enzymatically converted to d-lactate (dashed arrows on the right side). The grey arrows show increased production of AGEs and MG under hyperglycemic conditions. This leads to proinflammatory condition. Advanced glycation end product (AGE), adenosine triphosphate

(ATP), adenosine diphosphate (ADP), glucose-6-phosphate isomerase (G-6-P isomerase), Triphosphate intermediates (TPI)

1.5. Immune response after stroke and macrophage polarization

Inflammation (acute or prolonged) after ischemia is a self-regulating process in which microglia and infiltrated macrophages play an important role (Spite and Serhan 2010). There is an activation of microglia after stroke (Jin, Yang et al. 2010). Upon stimulation they behave like macrophages and perform different functions, including cytokine release, apoptosis, antigen presentation and matrix metalloproteinase (MMP) release. Many neurons in the ischemic penumbra may undergo apoptosis and may contribute to neurodegeneration (Okouchi, Ekshyyan et al. 2007; Broughton, Reutens et al. 2009). All these factors result in an impaired blood-brain barrier (BBB) (Wang, Tang et al. 2007; Iadecola and Anrather 2011). This allows infiltration of inflammatory cells, neutrophils, monocytes/macrophages and other immune cells. Neutrophils worsen the ischemic brain damage by producing iNOS, which increases the nitric oxide (NO) production and ultimately takes part in neurodegenerative processes (Dirnagl, Iadecola et al. 1999). The infiltration process is a cytokine-mediated process that also plays an important role in polarization of inflammatory monocytes (Ly-6C^{Hi}CCR2^{Hi} or M1 monocytes/macrophages) to non-inflammatory monocytes (Ly-6C^{Low}CCR2^{Low} or M2 monocytes/macrophages) (Dal-Secco, Wang et al. 2015). In mice, the earliest monocytes that migrate form bone marrow to the blood are inflammatory monocytes (M1 monocytes) (Passlick, Flieger et al. 1989). These macrophages migrate to different tissues and are named according to their anatomical location and/or on the basis of their phenotypes as described in the Figure 5 (Galli, Borregaard et al. 2011). In humans and mice, monocytes comprise two distinct sub-populations: classical monocytes and non-classical (alternate), and these cells are present in spleen, liver and circulation (Ingersoll, Platt et al. 2011). The classification of these subsets of monocytes is also explained on the basis of their expression of different surface markers (Mosser and Edwards 2008; Auffray, Sieweke et al. 2009).

The role of these monocytes/macrophages is tissue-specific and their functions are regulated by different signals originating from the tissue (Gordon and Taylor 2005; Murray and Wynn 2011). Monocytes/macrophages express chemokine receptors and pathogen recognition receptors that facilitate the migration of these cells from circulation to the tissues involved by inflammation (Serbina, Jia et al. 2008). Chemokines are a large group of proteins that attract leukocytes. CCL2 is the main chemokine that attracts monocytes/microglia to the site of injury (McTigue, Tani et al. 1998). The receptor for chemokine is CCR2 that interacts with CCL2 produced from microglia during the ischemic conditions and promotes the recruitment of inflammatory monocytes/macrophages.

Figure 5 Macrophage populations

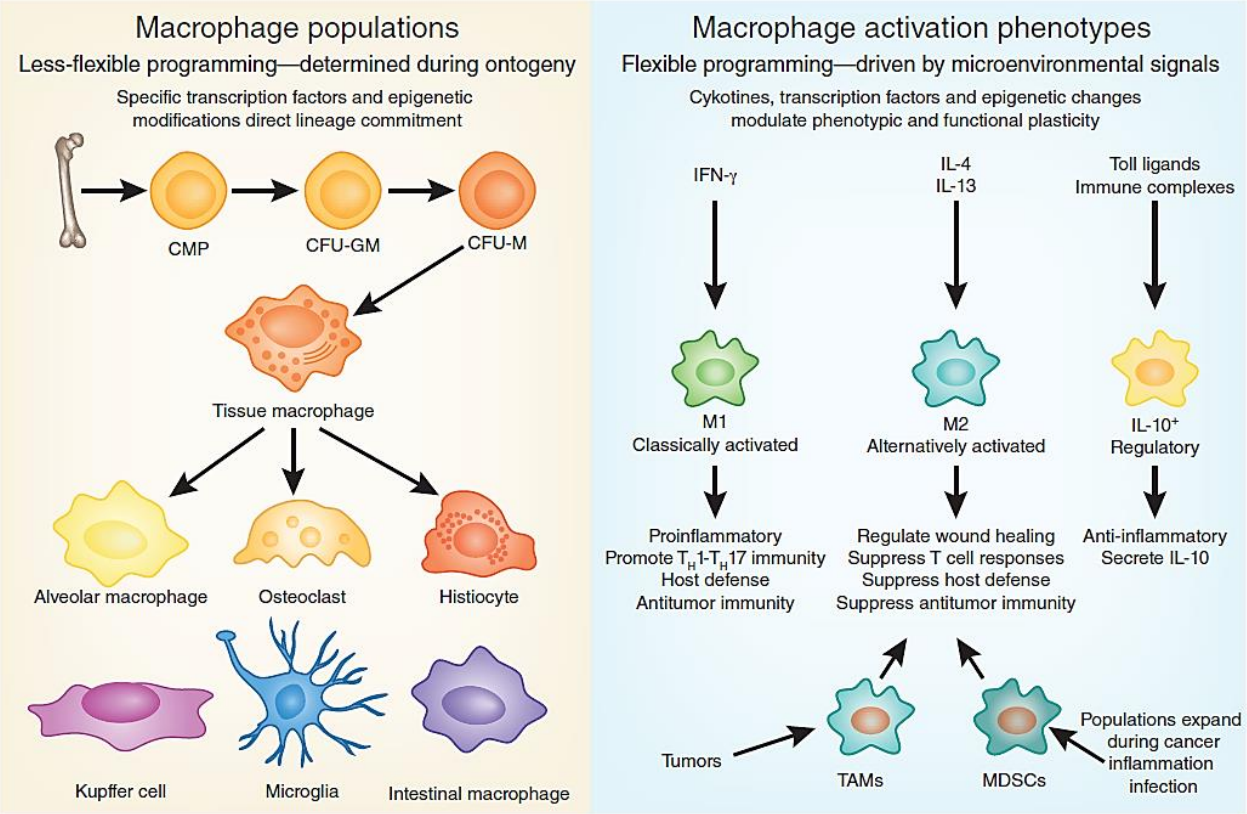

Functional subsets of macrophages. Figure adopted from Galli, Borregaard et al. 2011 (Galli, Borregaard et al. 2011). Macrophages can be classified based on their structural location (left) or functional phenotypes (right). Mononuclear phagocyte can also differentiate into tissue macrophages after entering different anatomical sites (for example microglia in the brain). Depending upon the stimuli these cells can be polarized into M1, M2 macrophages or Il-10 regulatory cells. Common myeloid progenitors (CMP), granulocyte/macrophage colony-forming unit (CFU-GM), myeloid colony-forming units (CFU-M), Interferon gamma (IFN-γ), Interleukin-4 (IL-4), Interleukin-13 (IL-13), Interleukin-10 (IL-10), Tumor-associated macrophages (TAMs), myeloid-derived suppressor cells(MDSCs).

1.6. Aims and objectives

The polarization of monocytes/macrophages is mediated by the release of chemokines and their interaction with specific receptors. Hyperglycemic conditions may interfere with the polarization of these cells consequently leading to an increased damage of the brain after stroke.

In this study, we aimed to investigate effects of hyperglycemia on the role of monocytes/macrophages in cerebral ischemia with the following intentions:

1. To establish a model of hyperglycemic stroke by inducing permanent occlusion of middle cerebral artery (MCAO), under normoglycemic (NG) and hyperglycemic conditions (HG).
2. To investigate the effect of hyperglycemic stroke on brain-infiltrating immune cells.
3. Does hyperglycemia affect the polarization of monocytes/macrophages after stroke?
4. Does ablation of CD11b positive monocytes/macrophages has an effect on infarct volume?
5. To explore the effect of AGE-RAGE interaction on infarct volume during hyperglycemia.

2. MATERIALS AND METHODS

2.1. Materials

2.1.1. Chemicals and commercial kits

Sr. No.	Chemical	Company
1	2,2,2-Tribromoethanol 97%	Sigma-Aldrich, Germany
2	2-Methyl-2-butanol	Sigma-Aldrich, Germany
3	Acetone	J.T.Baker, Netherlands
4	Ammonia solution 25%	Merk, Germany
5	Ammonium chloride	Merk, Germany
6	Bepanthen® (Eye ointment)	Bayer, Germany
7	BSA (Albumin, Fraction V)	Roth, Germany
8	Flow cytometer cleaning solution	Partec
9	Collagenase A	Roche, Germany
10	Diazabicyclo octane (DABCO)	Roth, Germany
11	Flow cytometer decontamination solution	Partec, Germany
12	DNAse I	Roche, Germany
13	Dulbecco's modified eagle medium (DMEM)	Invitrogen, Germany
14	Dulbecco's phosphate buffered saline (dPBS)	Biowest, USA
15	Formaldehyde solution 37%	Roth, Germany
16	Glucose monohydrate solution 50%	B.Braun, Germany
17	Hydrochloric acid, HCl 37%	Merck, Germany
18	Hydroquinone ≥ 99% (HPLC)	Fluka Chemika, Switzerland
19	Hypochlorite solution for flow systems	Partec, Germany
20	Isotonic sodium chloride	Diaco, Trieste, Italy

21	Lithium carbonate (Li_2CO_3)	Riedel-de Haën, Germany
22	Mowiol-488	Roth, Germany
23	Percol Plus	GE Healthcare
24	Paraformaldehyde	Merck, Germany
25	Ringer's solution	Berlin-Chemie, Germany
26	Sheath fluid for flow systems	Partec, Germany
27	Silver nitrate ≥ 99.9% $AgNO_3$	Roth, Germany
28	Sodium citrate di hydrate	J.T.Baker, Deventer, Netherlands
29	Tissue freezing medium (Jung)	Leica Microsys, Germany
30	Ethylene diamine tetra acetic acid (EDTA)	Roth, Germany
31	Tri-sodium citrate-2-hydrate	Riedel-de Haën, Seelze,Germany
32	Tween 20	Sigma-Aldrich, Germany

2.1.2. List of antibodies

Sr. No	Antibody	Company
1	Alexa Fluor 488 donkey anti-rabbit. IgG (H+L)	Life Technologies, USA
2	Anti Iba1, rabbit	Wako, Osaka, Japan
3	Anti-mouse CD45 PE , clone 30-F11	eBiosciences, SanDiego
4	Anti-mouse CD45 PerCP, clone 30-F11	BD Pharmingen
5	Anti-mouse Ly-6C APC, clone HK 1.4	Biolegend, San Diego
6	Anti-mouse Ly-6C PE-Cy™7, clone AL-21 (RUO)	BD Pharmingen
7	Anti-mouse CD11b APC, clone ML1/70	BD Biosciences
8	APC Rat IgG2c, k, isotype control clone RTK 4174	Biolegend, San Diego
9	Arginase I antibody (N-20) goat	Santa Cruz, USA
10	Cy3 donkey anti-goat IgG (H+L) anti-goat	JacksonImmuno Research
11	4,6-diamidino-2-phenylindole (DAPI)	Sigma-Aldrich, Germany
12	FITC anti-mouse Ly-6G, clone 1A8	BD Biosciences, Belgium
13	FITC rat IgG2a, isotype control	BD Biosciences, Belgium
14	PE rat IgG2b, isotype control	eBiosciences, San Diego
15	PE-Cy™7 rat IgM, k, isotype control	BD Biosciences
16	PerCP anti-mouse CD11b, clone M 1/70	Biolegend, San Diego
17	PerCP rat IgG2b, k, isotype control clone RTK4530	Biolegend, San Diego
18	Rat anti-mouse CD16/32, clone 2.4G2	BD Biosciences

2.1.3. Equipment and instruments

Sr. No.	Equipment /instrument	company
1	15 ml syringe	BD Discardit™ II, Spain
2	Bipolar forceps classic, angled, pointed	Erbe, Tübingen
3	Cell strainer (40-µm Nylon)	Falcon
4	Cell Trics (30-µm cell strainer)	Partec, Germany
5	Confocal microscope (TCS SP5)	Leica, Germany
6	Cotton applicator	Noba, Germany
7	Cryostat (CM 3050 S)	Leica, Germany
8	Electric coagulator (with a paddle switch) ICC50	Erbe, Tübingen
9	Eye needle (1/2 circle) HS-17	Serag Wiessner, Germany
10	FACSaria-III	BD Bioscience
11	Filter $597^{1/2}$ folded filters	S&S, Dassel, Germany
12	Flow cytometer (Cube8)	Partec, Germany
13	Fluorescence microscope (DMI 6000 B)	Leica, Germany
14	FMI-temperature-control module (TKM-0904)	FMI, Beerbach, Germany
15	Glucometer (Ascensia ELITE)	Bayer, Germany
16	Glucose measuring strips (Elite sensor)	Bayer, Germany
17	Magnetic stirrer (Ika-Combimag Ret)	IKA
18	Microliter syringe (1000 µl)	BD, Madrid, Spain
19	Microscope (SM 33)	Hund Wetzlar, Germany
20	Omnifuge 2. ORS (centrifuge)	Heraeus spatech
21	Paper tape 2-6205	neoLab
22	pH meter	WTW

23	Polysine slides (Thermo Scientific)	Thermo Scientific
24	Röhren tubes 3.5 ml, 55x12 mm,PS	Sarstedt, Nümbrecht, Germany
25	Safety-Multifly®- Set 21 G x ¾ TW	Sarstedt, Nümbrecht, Germany
26	Scanner CanoScan 9000 F	Cannon, Krefeld, Germany
27	Silk black (H4F) 3/0 USP	Resorba, Germany
28	Small volume sample tubes (1 ml)	Partec, Germany
29	Syringe needles 27G ¾ -Nr.20	BD Microlance™3
30	Water bath	B.Braun, Melsungen, Germany

2.1.4. Computer hardware and software

Sr. No.	**Hardware / Software**
1	Dell, OptiPlex 7010, 64-bit operating system, Intel(R) Core(TM) i5-3470 CPU
2	Windows 7 Ultimate, service pack 1
3	Windows XP
4	MS office 2010
5	Graph Pad Prism5
6	Flow Jo Version-X.0.6
7	Image J/ Fiji
8	End Note X5
9	Adobe Illustrator CC
10	Adobe Photoshop CC

2.2. Methods for animal experiments

2.2.1. Experimental animals

For all the experiments in this work, experimental animals were age- and gender-matched between groups. All experiments were conducted according to the German animal protection regulations and sanctioned by the local animal welfare authorities (Ministerium für Energiewende, Landwirtschaft, Umwelt und ländliche Räume, Kiel, Germany). In all the experiments 8- to 12-week-old mice were used. Experimenter was blinded for the treatment- and genotype- of groups before the start of each experiment. The sample size was calculated on the basis of the effect size (ε) calculations by dividing the difference in means (Δ) by the standard deviation (σ).

The following formula was used to calculate sample size:

$$\varepsilon = \Delta / \sigma$$

To measure the infarct volume, under normoglycemic (NG) and hyperglycemic (HG) conditions, C57BL/6 male mice (10-12 weeks) were used. Similarly, for flow cytometric analysis of immune cells infiltrating the brain, C57BL/6 and *Hca2*^{mRFP} (*Gpr109a*^{mRFP}) mice were used (Hanson, Gille et al. 2010). To test the effect of monocyte-depletion on infarct volume CD11b-DTR mice were utilized. To explore the involvement of the receptor for advanced glycation end products (RAGE) in ischemic brain damage under NG and HG conditions, RAGE$^{-/-}$ mice were used. RAGE$^{-/-}$ mice were kindly provided by Dr. Thomas Fleming and Prof. P. Nawroth, University of Heidelberg. In-house bred, age-matched C57BL6/N mice were used as control because the RAGE $^{-/-}$ were 18 times backcrossed with C57BL6/N. Breeding pairs of C57BL6/N mice were purchased from Charles River, Germany.

2.2.2. Preparation for surgery

The surgical instruments were sterilized with 70% ethanol. Pentobarbital (0.075-0.01 mg/g) was used as an anesthetic agent (Weiss and Zimmermann 1999). The anesthetic agent was prepared by diluting commercially available pentobarbital (96 mg/1.8 ml) with sterile PBS and the stored the diluted solution at 4° C in a light-protected bottle. The final concentration of the pentobarbital solution was 5 mg/ml. All mice were kept in 37 x 19 x 12-cm (length x width x height) cages at 20-24 °C and 50-70% humidity.

2.2.3. Preparation of 4% paraformaldehyde (PFA)

PFA (40 g) was mixed with 2.5 ml of NaOH (1N; 40 g NaOH per 1000 ml) and PBS (800 ml). This solution was heated to 70° C. The solution was left for a while to cool down and the pH was adjusted to 7.4. The final volume was made up to 1000 ml by adding water. Aliquots of the solution were stored at -20° C in the 50-ml Falcon tubes.

2.2.4. Preparation of diphtheria toxin (DT)

Diphtheria toxin (1 mg) was diluted with distilled water (1 ml). Aliquots of 50 µl were kept at -20° C. For injecting, a 50 µl aliquot was diluted with 10 ml of sterile PBS. Diphtheria toxin (25 ng per gram body weight) was administered intra-peritoneal (i.p).

2.2.5. Bone marrow transplantation

Bone marrow transplantation (BMT)* was performed as described previously (Muhammad, Barakat et al. 2008) with the following modifications. Mice were killed by cervical dislocation, and bone marrow was aseptically collected from femurs and tibias. Unfractionated bone marrow cells were resuspended in 0.25 ml sterile PBS and injected retro-orbitally into 10- to 13-week-old C57BL/6 and Hca2^{mRFP} mice that had been lethally irradiated (dose of 10 Gy in 2 divided sessions, 5 Gy each time with a 4-hours interval, 10 MV- bremsstrahlung, dose rate of 3 Gy / min) 1 day before. Six weeks after reconstitution, mice were subjected to MCAO. Flow cytometry of blood cells was performed before and 24 hours after MCAO, while flow cytometry of the brain cells was performed 24 hours and 48 hours after MCAO.

* Preparation and radiation of the recipient mice was done by me. Preparation of bone marrow cells was performed by Dr. Dirk A. Ridder and Dr. Hui Chen. Six weeks after BMT, MCAO and flow cytometry of blood and brain was performed by me. Cryosection, immune staining, calculation and analysis of flow cytometry data were done by me.

2.2.6. Blood glucose measurement

Blood glucose concentrations were measured after anesthetizing the mice from the tail. A marginal difference in glucose concentration has been reported between blood samples obtained from the retro-orbital or tail vein (Rogers, Holder et al. 1999). A small cut was made on the tip of the tail. A drop of blood was transferred directly on the glucose measuring strip (Elite sensor, Bayer). The concentration was noted in milligram per deciliter (mg/dl). Blood glucose concentrations were measured at three time points. The first measurement was performed immediately after anesthetizing the mice (0 minute), the second measurement after 30 minutes and the third one after 50 minutes of the first measurement.

Figure 6 Experiment protocol

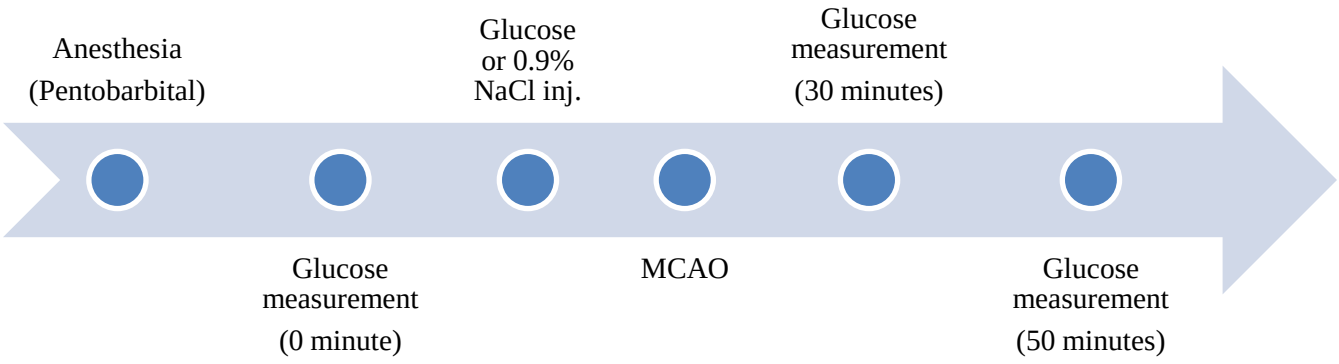

To induce hyperglycemia, 200 µl of 25% glucose solution was administered i.p, while in control mice; an equal volume of 0.9% NaCl was injected.

0.9% sodium chloride (0.9% NaCl), Middle cerebral artery occlusion (MCAO), Injection (inj)

2.2.7. Middle cerebral artery occlusion (MCAO) surgery

MCAO was performed as described previously (Bargiotas, Muhammad et al. 2012).The mice were anesthetized with an i.p injection of pentobarbital (0.075-0.1 mg/g body weight). One-2 minutes after injection, the hind limb paw was pressed with the finger to confirm that the mice were under adequate anesthesia. During the whole surgical procedure, its body temperature was maintained between 37° C to 37.5° C by a rectal thermometer controlling the heating pad. An eye ointment (e.g., 5% dexpanthenol (Bepanthen®) was administered to protect both eyes. The skin was disinfected with 70% ethanol. Under a surgical microscope (SM33 Hund Wetzlar, Germany), a skin incision of 2-4 cm was made between the left orbit and tragus to expose the temporal muscle. The temporal muscle was removed with the help of a microbipolar electrical coagulator (Erbe, 20195-013). After the removal of the temporal muscle, the bifurcation of the MCA was visible under the skull, indicating the site of craniotomy. Some drops of 0.9% NaCl were added and drilling was started on the skull. For drilling a dental drill (Proxxon, 41415-2008) was used at a speed of 10-17 thousand cycles per minute. When a circular hole with a diameter of about 2 mm was drilled, the dura was exposed and it was removed carefully with a fine forceps. The left distal MCA (dMCA) was occluded below and above the bifurcation with an electrical coagulator. Occlusion was done at three sites to ensure that it is irreversible. The wound was closed by stitching the skin with black silk (3/0 USP) using a half circle needle (HS-17). Then mice were kept under red light for approximately 15-20 minutes and returned to the home cages. After MCAO surgery, the mice were observed two times a day till perfusion was done.

Figure 7 Steps of MCAO surgery

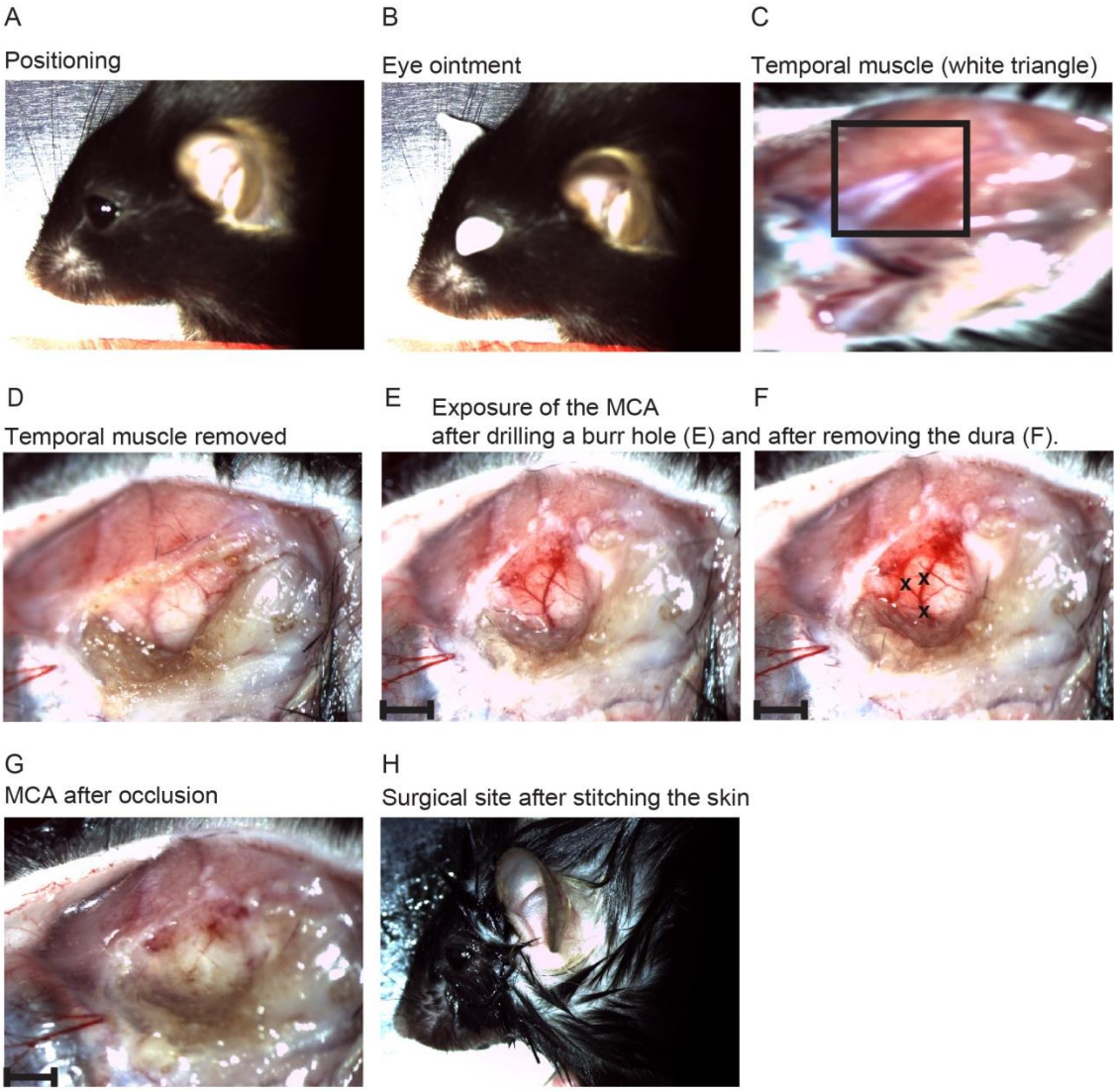

(A-H) Different steps of the MCAO surgery. (A, B) Positioning the mouse and administration of an eye-ointment. (C) Temporal muscle exposed, shown in the black square. (D) Bifurcation of MCA visible after removal of the temporal muscle. (E) The burr-hole drilled in the skull.to expose the MCA (F, G) Dura removed and occlusion of the MCA performed at the points marked with 'X' in figure F.(H) Wound closed after stitching.

For figurres E-G, Sclae bar, 1 mm. Middle cerebral artery (MCA), Middle cerebral artery occlusion (MCAO)

2.2.8. Perfusion and removal of the intact brain

Two days after MCAO, the mice were reanesthetized with 2.5% TBE given i.p. at a dose of 20 µl/g body weight. The mice were fixed on a thermopore sheet in a supine position. The thoracic cavity was opened, an 18G ¾ butterfly needle was inserted through the left ventricle into the ascending aorta. After opening the right atrium the mice were perfused by injecting 15-20 ml Ringer's lactate buffer at a constant pressure. After perfusion, the brain was exposed and carefully dissected without damaging its surface. The brain was kept on dry-ice and then stored at -20° C or -80° C in a well labelled plastic container.

2.2.9. Cryosectioning

For cryosectioning a temperature of -20° C and a section thickness of 20 µm were used. A small volume of tissue freezing medium was dropped on the specimen disc and the brain was positioned vertically. The specimen disc was placed on the quick freeze shelf inside the cryostat. The whole brain was covered with tissue freezing medium and was placed inside the cryotome until it was completely frozen.

In the meantime, the slides of series-1 (S1) to series-3 (S3) were labelled with adequate information about the experiment. The specimen disc and the blade were fixed. The olfactory bulb was trimmed, and 20 µm thick sections of each series S1 to S3 were collected on slides. A distance of 400 µm was maintained between two consecutive sections on each slide. In this way usually 23-24 sections per brain were obtained. The slides were stored at -20 ° C or -80 ° C in well-labelled plastic boxes. Series-1 (S1) was dried at room temperature before the start of silver staining.

2.2.10. Silver staining

Impregnation and developing solutions were prepared.

2.2.10.1. Impregnation solution

For 60 slides, 3.375 g $AgNO_3$ was dissolved in 33.75 ml H_2O (10% w/v $AgNO_3$). In a separate conical flask, 67.5 ml H_2O was added to 0.81 g $LiCO_3$ to make a suspension. Then, 10% $AgNO_3$ was mixed with the $LiCO_3$ suspension (color turns yellowish). Ammonia solution (25 %) was added drop by drop until a gray solution was reached (maximum volume 3.6 ml). Finally, 506.25 ml water was added.

N: An excess of ammonia was avoided because it would disturb.

2.2.10.2. Developer solution

In a 1000 ml conical flask, 1.8 g hydroquinone and 6.6 g Sodium citrate were dissolved in filtered 37% formaldehyde solution (120 ml). Then, acetone (90 ml) and H_2O 420 ml were added. The flask was wrapped with aluminum foil to protect from light. The solution was mixed with a magnetic stirrer for about 1 h until its color turned to a light red. The slides were incubated in the impregnation solution for 2 minutes and washed three times for 1 minute with aqua dest. Then the slides were placed in the developing solution for 2-3 minutes and again washed with aqua dest three times for 1 minute. Before scanning, the stained slides were dried overnight at room temperature.

2.2.11. Scanning

A small scale was fixed at one side of the scanner. Slides from series 1 (S-1) were put next to this scale in an inverted position. After scanning the images were saved in TIF format using grey scale and a resolution of 300 dpi.

2.2.12. Method for the infarct size measurement

A computer program (ImageJ) was used to measure the area of silver deficit, the right hemisphere, and the left hemisphere on all sections. Sections without silver deficit were also analyzed.

The infarct area was calculated for each section with the following equation:

Right hemisphere + silver deficit – left hemisphere = Infarct area

Edema was calculated with the following equation:

Left hemisphere – right hemisphere = Edema

The infarct volume was calculated by adding the infarct areas and multiplying the sum by the distance between sections. In the same way, the edema volume was calculated.

2.3. Methods for flow cytometry experiments

2.3.1. Preparation of fluorescence activated cell sorting (FACS) solutions

2.3.2. FACS buffer

BSA (2.5 g) and NaN_3 solution (1.54 ml, 1 M) were mixed in PBS (500 ml).

One molar NaN_3 solution: Sodium azide (NaN_3, 3.2505 g) was dissolved in 50 ml of PBS.

2.3.3. Digestion buffer

Collagenase-A (100 mg) and DNAse (10 mg) were diluted in 100 ml of DMEM. Aliquots were stored at -20° C in 5-ml Falcon tubes.

2.3.4. Erythrolysis buffer

NH_4Cl (8.02 g), $KHCO_3$ (1 g), Na_2EDTA (0.037 g) were dissolved in deionized water and the final volume was adjusted to 1000 ml. The pH was adjusted to 7.2 – 7.4.

2.3.5. Phosphate buffered saline (PBS) 10x (1 L)

NaCl (80.0 g), KCl (2.0 g), $Na_2HPO_4.7H_2O$ (26.8 g), KH_2PO_4 (2.4 g) were added in 1000 ml of H_2O. The pH was adjusted to 7.4.

2.3.6. Preparation of Percol (90%)

Percol-plus (90 ml) and 10x PBS (10 ml) were mixed and stored at 4° C.

2.3.7. Preparation of Percol-A (78%)

Forty seven milliliters of 90 % Percol were diluted with 1x PBS (13 ml) and stored at 4° C.

2.3.8. Preparation of Percol-B (30%)

Twenty milliliters of 90% percol were added to 40 ml of DMEM and stored at 4° C.

Note: All the containers were well labeled and tightly closed.

2.4. Procedures

2.4.1. Brain cell preparation

Before starting the cell preparation, the water bath was turned on to attain a temperature of 37° C, and the centrifuge was cooled down to 4° C. The digestion medium was thawed and the other required materials were prepared.

2.4.1.1. Perfusion and collection of brain

The mice were deeply anesthetized with TBE (2.5%) by administering a dose of 20 µl/g. After perfusion with 15 ml Ringer's solution, the brains were collected and the cerebella and olfactory bulbs were removed. The brains were divided into left and right hemispheres for cell preparation. Then, the tissue was collected into a petri dish containing ~5 ml PBS until all the brains were removed. The hemispheres were transferred into another dry petri dish and a drop of digestion medium was added. The hemispheres were cut it into small pieces. Digestion medium (~1 ml) was added and transferred with the tissue into 50-ml Falcon tubes with a 10-ml pipette. The remaining 4 ml of the digestion medium aliquot was also added in the 50-ml Falcon tubes. The Falcon tubes with brain tissue suspension were incubated in a shaking water bath at 37° C for 30 minutes. The brain tissue was homogenized thoroughly with a 10-ml pipette. The digested tissue was passed through a 40-µm nylon cell strainer (BD Biosciences). The cell strainer was washed with 40 ml cold PBS. The cell suspension was centrifuged at 310 g for 10 minutes at 4° C.

2.4.1.2. Preparation of cells

The cell pellet was resuspended in 5 ml erythrocyte lysis buffer and was incubated for 7 minutes on ice to lyse the red blood cells (RBCs). The Falcon tubes were filled with cold PBS and centrifuged at a speed of 310 g for 10 minutes at 4° C. After centrifugation the supernatant was discarded and the cells were resuspended in 2.8 ml percoll B (30%). The suspension was transferred to another 15-ml Falcon tubes. A 5-ml pipette was slowly advanced to the bottom of the tube and percoll B underlied with percoll A (2.5 ml)**.** The weight of the tubes was balanced (if necessary) with percoll B**.** The Falcon tubes were centrifuged (without brake, Decel = 0) at 1350 g for 30 minutes at 4° C. The cells were collected from the interface of the gradient with a 1-ml pipette and were transferred to fresh 15-ml Falcon tubes**.** The tubes were filled with FACS buffer and mixed gently by inverting. Then they were centrifuged at 700 g, 10 minutes and 4° C (brake turned on again). The cell pellet was washed 1-2 times with 10 ml of FACS buffer at centrifugation 310 g for 10 minutes at 4° C**.** The supernatant was discarded and the cells were resuspended in 100 µl FACS buffer.

2.4.1.3. Staining protocol

A first step was to determine the optimal antibody concentration and incubation time. The cell suspension (100 µl) was incubated on ice for 15 minutes with anti-mouse CD 16/32 (Fc-block, BD Pharmingen, 1 µl). Then, the cells were incubated with the antibodies or their respective isotype controls (1 µl for 100 µl cell suspension) for 45 – 60 minutes at 4° C in the dark.

2.4.2. Blood

The mice were anesthetized with an i.p injection of 2.5% TBE at a dose of 20 µl per gram body weight. Ten µl 0.5 M EDTA (sterile filtered) was aspirated into a syringe and was spread across the syringe walls by pipetting it up and down. The blood was collected from the inferior vena cava (alternatively: cardiac puncture) and kept in a shaker until the staining was performed. One-hundred µl of whole blood was incubated with antibodies (1 µl for 100 µl cell suspension) for 45 to 60 minutes at 4° C in the dark. The erythrolysis buffer (1 ml) was added and mixed gently. This mixture was then transferred to 15-ml Falcon tubes and were incubated for 7 minutes on ice. After adding PBS (4 ml) the whole suspension was centrifuged at a speed of 310 g for 10 minutes at 4° C. The supernatant was discarded carefully and of FACS-buffer (400 µl) was added before analyzing with the flow cytometer (Partec Cube 8).

2.5. Immune fluorescence microscopy

2.5.1. Preparation of solutions

2.5.1.1. Preparation of 30% sucrose

Sucrose (30 g) was dissolved in 100 ml of PBS.

2.5.1.2. Preparation of the citrate buffer

Sodium citrate (2.94 g) was mixed in 1000 ml H_2O and the pH was adjusted at 6.

2.5.1.3. Preparation of 0.05% Tween-20

Tween-20 (500 µl) was dissolved in 1000 ml of 1x PBS (PBST).

2.5.1.4. Preparation of 5% and 10% BSA

For a 10% BSA solution, BSA (10 g) was dissolved in 100 ml of PBST. To prepare a 5% dilution, 10 % BSA was diluted with an equal volume of PBST.

BSA (10 %) was used as blocking solution and 5 % BSA was utilized for the preparation of antibody dilutions.

2.5.1.5. Preparation of Mowiol

Poly (vinyl alcohol)/Mowiol® 488 (2.4 g, 10% W/V), glycerol (6g, 25% W/V), water (6 ml) and Tris-buffer (12 ml, 0.2 M, pH 8.5) and 0.1 % DABCO (Roth) were mixed for 24 hours. Then, the mixture was centrifuged for 15 minute at a speed of 6198 g. The aliquots of supernatant were stored at - 20° C.

2.6. Perfusion

Two days after the MCAO, the mice were reanesthetized and slowly perfused with 10 ml Ringer's lactate buffer followed by 10 ml 4% PFA. Post-fixation was done for 24 hours in 4% PFA at 4° C and the cryoprotection was done for 24 hours at 4° C in 30% sucrose. The brains were quickly frozen in the super-cooled isopentane and then the brains were transferred on dry ice. The brains were stored at -70° C to -80° C. Before cryosectioning the brains were maintained at -20° C for 30 minutes. The cryosections of 20-µm thickness were used for immune staining and the slides were stored at -20° C or -70° C.

2.7. Staining

After drying the frozen sections for 1 hour, a rectangle was drawn around the sections with an ImmEdge Pen (Vector). The slides were rehydrated in 1x PBS for 5 minutes. For antigen retrieval, citrate buffer was heated to 98° C. When the temperature dropped to 92° C at room temperature, then the slides were incubated in the buffer till its temperature dropped to 35° C. The slides were washed three times in PBST for 5 minutes and kept in blocking solution (10% BSA in PBST) for 35 minutes. Arginase I (1:200) and Iba1 (1:100) antibodies dilutions were prepared in 5% BSA. The slides were incubated overnight (O/N) at RT with 250 µl of primary antibodies dilution. Next day, after washing with PBST, the slides were incubated with respective secondary antibodies (1:400) and DAPI (1:2000). Anti-goat Cy3 and anti-rabbit Alexa-488 were used as secondary antibodies for arginase I and Iba-1 respectively. Mounting medium was added after washing the slides with PBST. Imaging was performed on a fluorescence (DMI 6000 B, Leica) or a confocal microscope (TCS SP5, Leica) using the same settings for the whole experiment.

2.8. Statistical analysis

All data are illustrated as means ± SEM. Two groups were compared by using unpaired, two-tailed t-test. Three or more groups were statistically compared with two-way analysis of variance (ANOVA), followed by Bonferroni posthoc tests (GraphPad Prism 5.0 software). Values were considered to be significant at p-values <0.05.

3. EXPERIMENTS AND RESULTS

3.1. Sample size calculations

One of the most important features of planning a research project is the calculation of the sample size. In general the sample size depends on the acceptable level of significance, power of the experiment, estimated effect size and standard deviation of the population (Kirby, Gebski et al. 2002). In this study, the sample size was calculated on the basis of effect size (ε) calculated by dividing the difference in means (Δ) by the standard deviation (σ).

The following formula was used to calculate the effect size:

$\varepsilon = \Delta / \sigma$

$\Delta = 7.28$ and $\sigma = 4.71$

$\varepsilon = 7.28 / 4.71 = 1.54$

Effect size (ε) = 1.54

The following table lists typical sample sizes for diverse effect sizes.

Table 1 Sample size estimation. The values are based on a power of 0.8 and p<0.05.

Effect size	t-Test	t-Test (one)	t-Test (two)	ANOVA 3 Gr.	ANOVA 4 Gr.	ANOVA 6 Gr.
0.8	15	21	26	31	35	41
0.9	122	16	21	25	28	33
1.	10	14	17	20	23	27
1.1	9	11	15	17	19	22
1.2	8	10	12	15	16	19
1.3	7	9	11	13	14	17
1.4	7	8	10	11	13	14
1.5	6	7	9	10	11	13

Student's t-test (t-Test), One-sample Student's t-test (t-Test (one)), Two-sample Student's t-test (t-Test 8two)), Analysis of variance with three groups (ANOVA 3 Gr.), Analysis of variance with four groups (ANOVA 4 Gr.), Analysis of variance with six groups (ANOVA 6 Gr.).

The effect size 1.54 corresponds to the sample size 11 in the column of ANOVA with 4 groups. Therefore, we used 11 mice in each group.

3.2. Establishment of a mouse model of hyperglycemic stroke

It is well established that preischemic hyperglycemia (HG) enhances ischemic brain damage in human as well as in animal models of both global and focal cerebral ischemia. Both experimental and clinical studies have shown that besides the susceptibility to stroke occurrence and the severity of brain damage, the likelihood of death from stroke are increased in persons with hyperglycemic conditions regardless of a preexisting diabetes. The molecular mechanisms underlying this important, clinically relevant phenomenon are not fully understood. Therefore, to find out the effect of hyperglycemia on infarct size we used an animal model of stroke in mice. The mean blood glucose levels were significantly higher in hyperglycemic groups than that of normoglycemic groups. The higher blood glucose levels were observed at both time points (30 minutes and 50 minutes) after glucose administration (Figure 8 A). Forty-eight hours after MCAO, the mice were anesthetized with TBE (20 µl per gram body weight), perfused with Ringer's solution and the brains were harvested. The infarct size was significantly higher in hyperglycemic mice than that of the mice in the normoglycemic group (Figure 8 B).

Figure 8 ***Hyperglycemia increases infarct volume.***

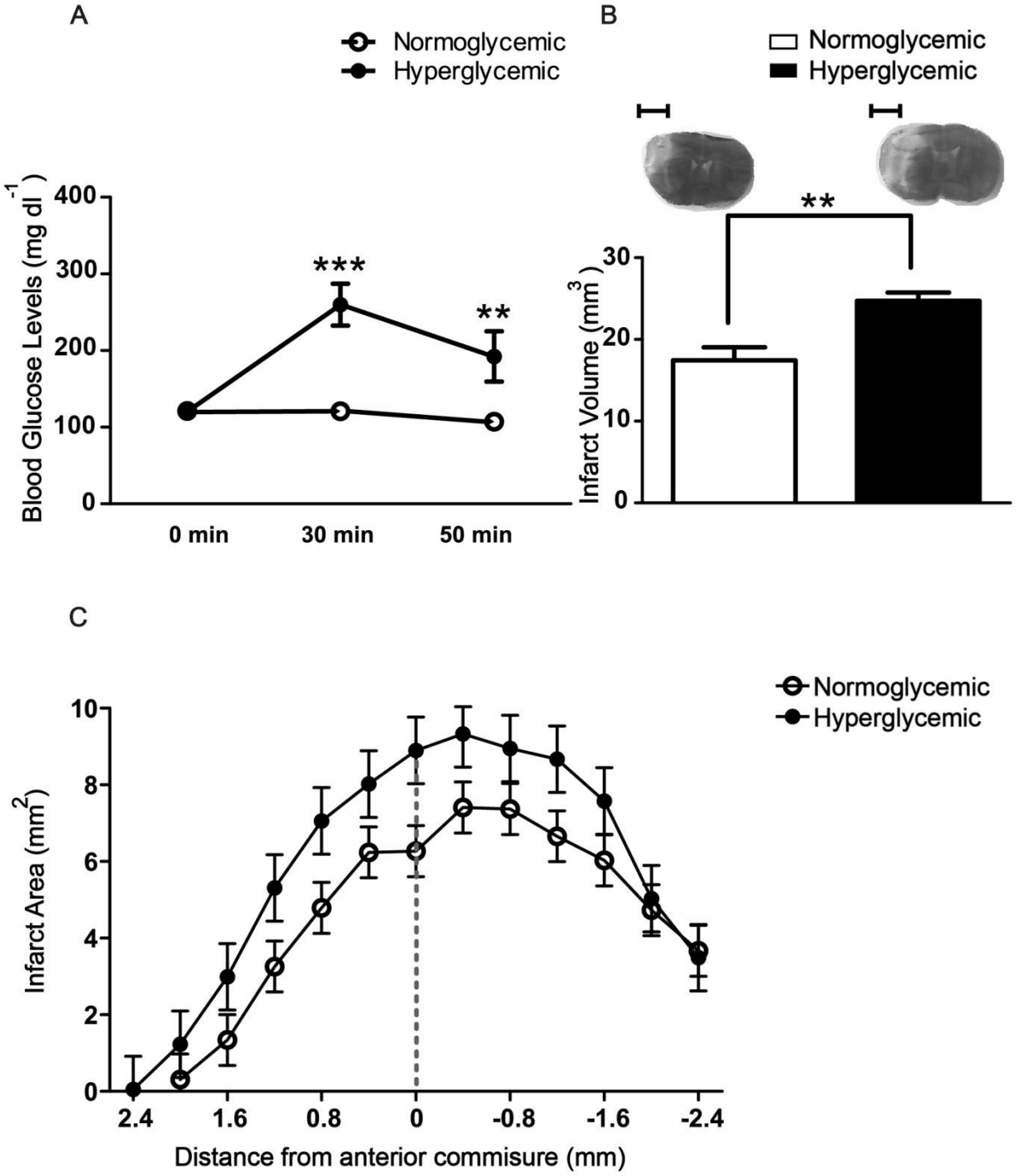

(A) Blood glucose concentrations were significantly increased when mice were treated with 200 µl of 25% glucose (0.05g). Blood glucose measurements were performed immediately after anesthesia (Zero minute), 30 minutes and 50 minutes after the glucose or normal saline

*injections. White circles for normoglycemic and black circles for hyperglycemic mice. MCAO was performed after the first measurement. Two-way ANOVA, *** p=<0.001. **p=<0.01 (Bonferroni posttests), values are mean ± SEM (n=11/group).*

*(B) Hyperglycemic group had higher infarct volume as compared to normoglycemic group. Unpaired t-test, **p<0.0016, values are mean ± SEM (n=13/group) scale bar= 2.5 mm*

(C) Distribution of infarct over coronal sections in normoglycemic (white circles line) and hyperglycemic groups (black circles).

3.3. BM-derived HCA_2-positive cells are M2 polarized macrophages

In our previous study, it was proved that the neuroprotective effect of nicotinic acid was mediated through the HCA_2 receptor. The expression of HCA_2 was localized in the brain, by using the BAC-transgenic mouse line *Hca2*^{mRFP} (*Gpr109a*^{mRFP}). Normally, mRFP was expressed exclusively by CD11b$^+$ microglia, but not by astrocytes and neurons. After MCAO, mRFP$^+$ cells accumulated along the periphery of the cortical ischemia. Based on the expression of CD11b and Iba1, HCA_2^+ cells were identified as microglia or monocytes/macrophages that infiltrated the ischemic brain. To categorize, these two cell populations, chimeric mice were used. Wild-type bone marrow was transplanted to *Hca2*^{mRFP} mice (WT>*Hca2*^{mRFP}) and *Hca2*^{mRFP} bone marrow to wild-type mice (*Hca2*^{mRFP}>WT). Flow cytometry was performed to characterize the sub-population of mRFP$^+$ cells. It was found that in the brain, mRPF was expressed largely by Ly-6C^{Lo} monocytes/macrophages (Figure 9). Bone marrow-derived mRFP$^+$ cells expressing CD11b were already detected 24 hours after MCAO in the ischemic brain of Hca2^{mRFP} > WT mice, but their number was higher 48 hours after MCAO (Figure 9). Further analysis confirmed that the bone-marrow derived brain infiltrated mRFP$^+$ cells were CD45$^+$CD11b$^+$Ly-6G$^-$, that confirmed their monocytic/macrophagic identity (Figure 9 F and G). In contrast, in blood mRFP$^+$CD45$^+$CD11b$^+$Ly-6G$^-$ monocytes were equally distributed between Ly-6C^{Lo} and Ly-6C^{Hi} subpopulations before MCAO (Figure 10). After MCAO, the number of Ly-6C^{Hi} monocytes reduced but Ly-6C^{Lo} monocytes remained unchanged (Figure 10).

Figure 9 Flow cytometric characterization of HCA_2-expressing cells in brain

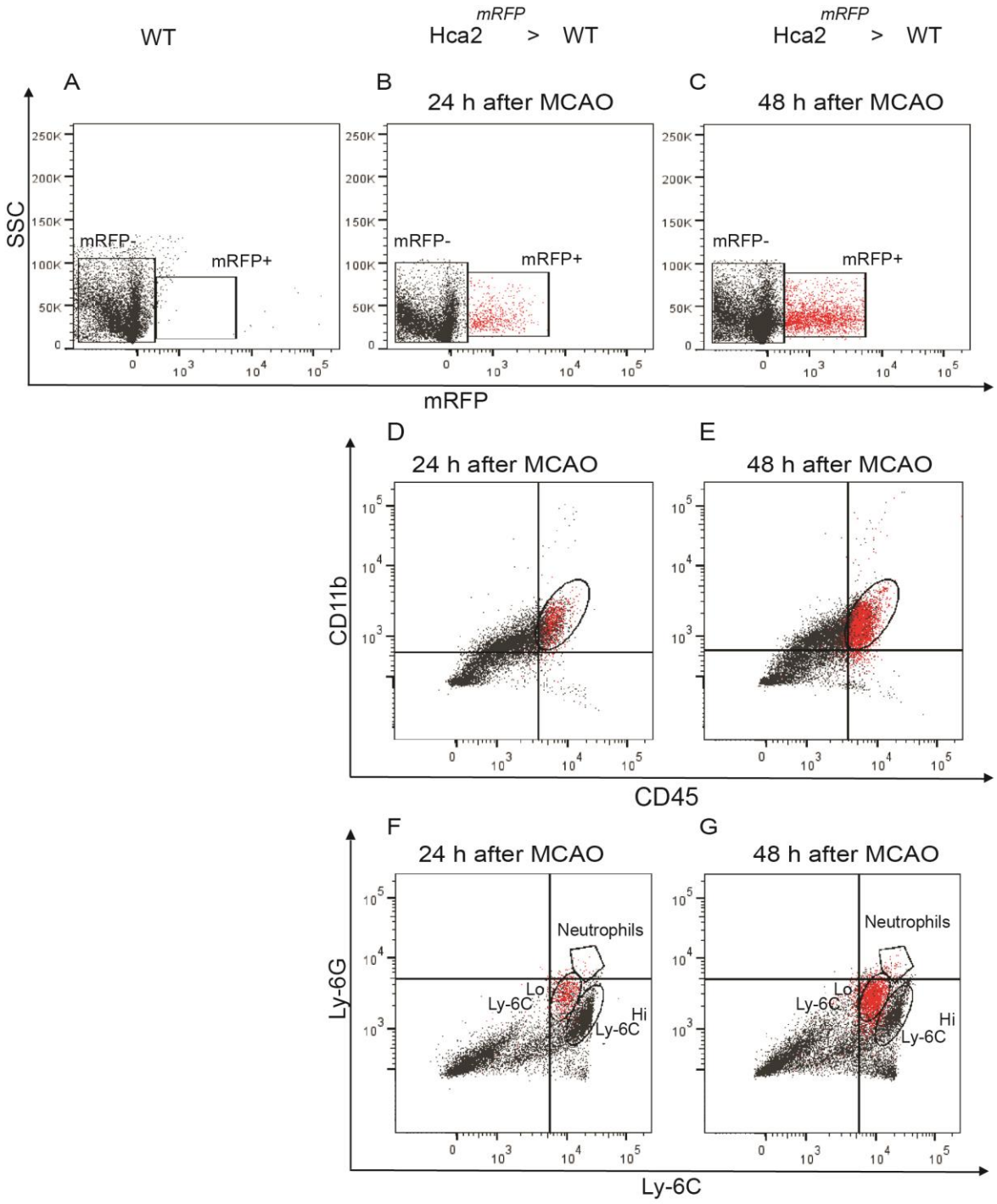

Flow cytometric characterization of HCA2-expressing bone marrow-derived cells in the ischemic brain. (A–C) Using flow cytometry after MCAO, we detected $mRFP^+$ cells in the brain of chimeric $Hca2^{mRFP}$>WT mice but not in wild-type (WT) animals. The number of $mRFP^+$ cells

increased between 24 hours and 48 hours after MCAO. Hca2^{mRFP}>WT mice were generated by transplanting Hca2^{mRFP} bone marrow to WT animals. (D, E) Gated mRFP^{+} (red dots) and mRFP^{-} (black dots) cells in the ischemic hemisphere were CD11b^{+}CD45^{+}. (F, G) Gated mRFP^{+} cells were mainly Ly-6C^{Lo} and Ly-6G^{-} in contrast to mRFP^{-} cells. Only CD45^{+}CD11b^{+} cells are shown.

Figure 10 Flow cytometric characterization of HCA_2-expressing cells in blood

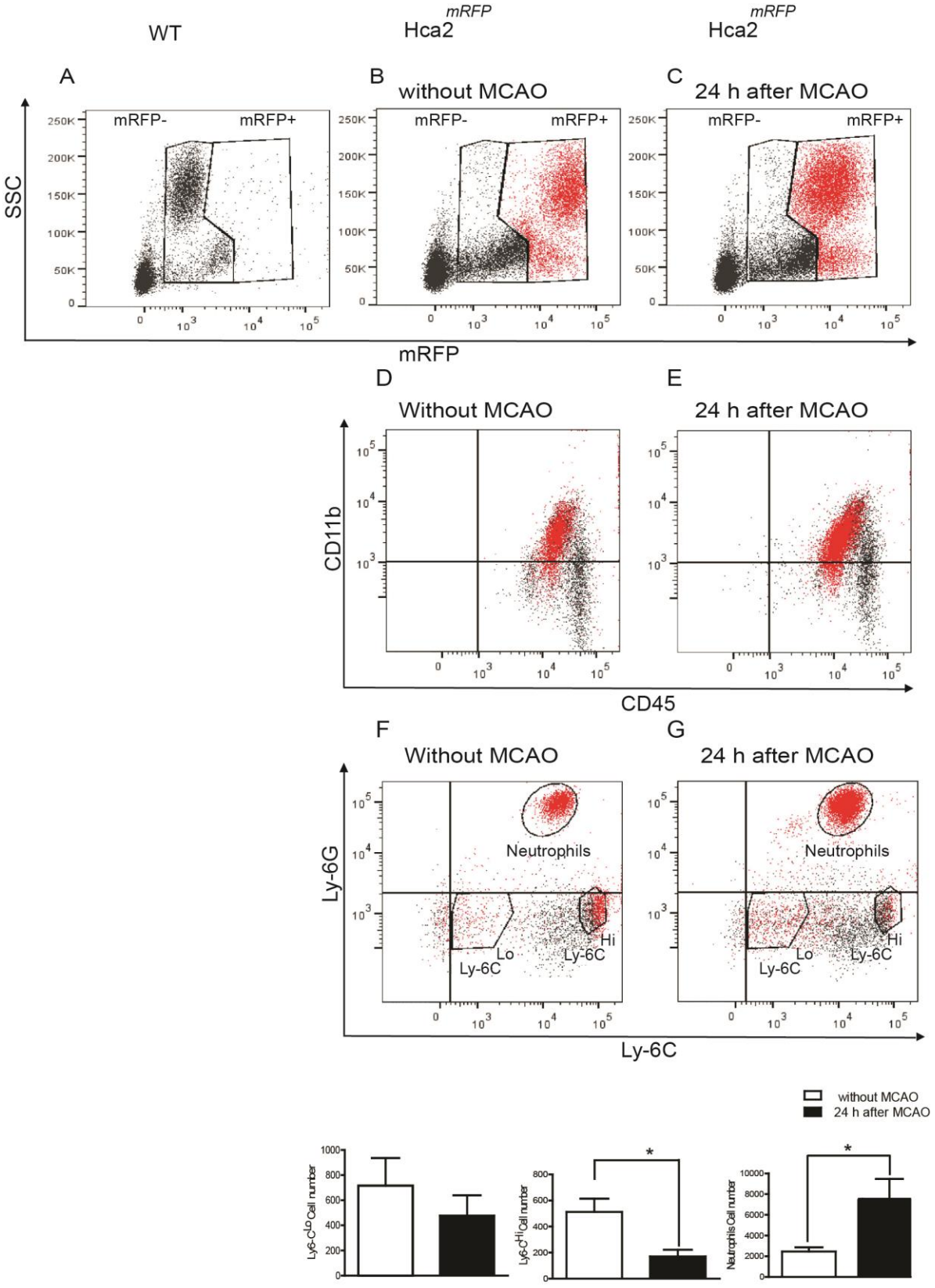

*Flow cytometric characterization of HCA2-expressing cells in blood. (A–C)We detected RFP^+ cells only in the blood of $Hca2^{mRFP}$mice before and 24 hours after MCAO. (D, E) Gated $mRFP^+$ (red dots) and $mRFP^-$ (black dots) cells were $CD11b^+CD45^+$. (F, G) Gated $mRFP^+$ cells fell into three populations: $Ly\text{-}6G^+$ (neutrophils), $Ly\text{-}6G^-Ly\text{-}6C^{Lo}$ and $Ly\text{-}6G^-Ly\text{-}6C^{Hi}$ monocytes. Only $CD45^+CD11b^+$ cells are shown. Quantification of $mRFP^+$ cells revealed an increase of neutrophils and a decrease of $Ly\text{-}6C^{Hi}$ monocytes 24 hours after MCAO. Values are means ± S.E.M (n=6). *P<0.05 (unpaired t-test).*

3.4. Hyperglycemia downregulates M2 monocytes/macrophages

These findings increased the curiosity whether hyperglycemia would affect brain infiltrating immune cells. We investigated the effect of hyperglycemia on these cells by flow cytometry. MCAO was performed in wild-type mice under normoglycemic and hyperglycemic conditions. Forty-eight hours after MCAO surgery, the brains were collected and immune cells were prepared from brains. The cells were stained with CD45 PE, CD-11b PerCP, Ly-6C APC and Ly-6G FITC antibodies. Flow cytometry was performed on these cell-preparations and the cell populations were gated against CD45 and CD11b. The $CD45^{+}CD11b^{+}$ cells were distributed into two distinct $CD11b^{+}CD45^{Low}$ and $CD11b^{+}CD45^{Hi}$ subsets (Figure 11 B, E). These subsets of CD45 were further gated, against Ly-6C and Ly-6G. $CD45^{Lo}$ cells, consisted of a single population of $Ly\text{-}6C^{Lo}$ cells (Figure 11 C, F). In contrast among $CD45^{Hi}$ cells, three distinct sub-populations of $Ly\text{-}6C^{Lo}$, $Ly\text{-}6C^{Hi}$ and neutrophils could be distinguished. Interestingly, the number of $CD45^{Hi}CD11b^{+}Ly\text{-}6G^{-}Ly\text{-}6C^{Lo}$ (M2 monocytes/macrophages) was reduced under hyperglycemic conditions. However, the numbers of $CD45^{Lo}Ly\text{-}6C^{Lo}$, $CD45^{Hi}Ly\text{-}6C^{Hi}$ and neutrophils remained unaffected (Figure 12).

Figure 11 Hyperglycemia downregulates M2 macrophages.

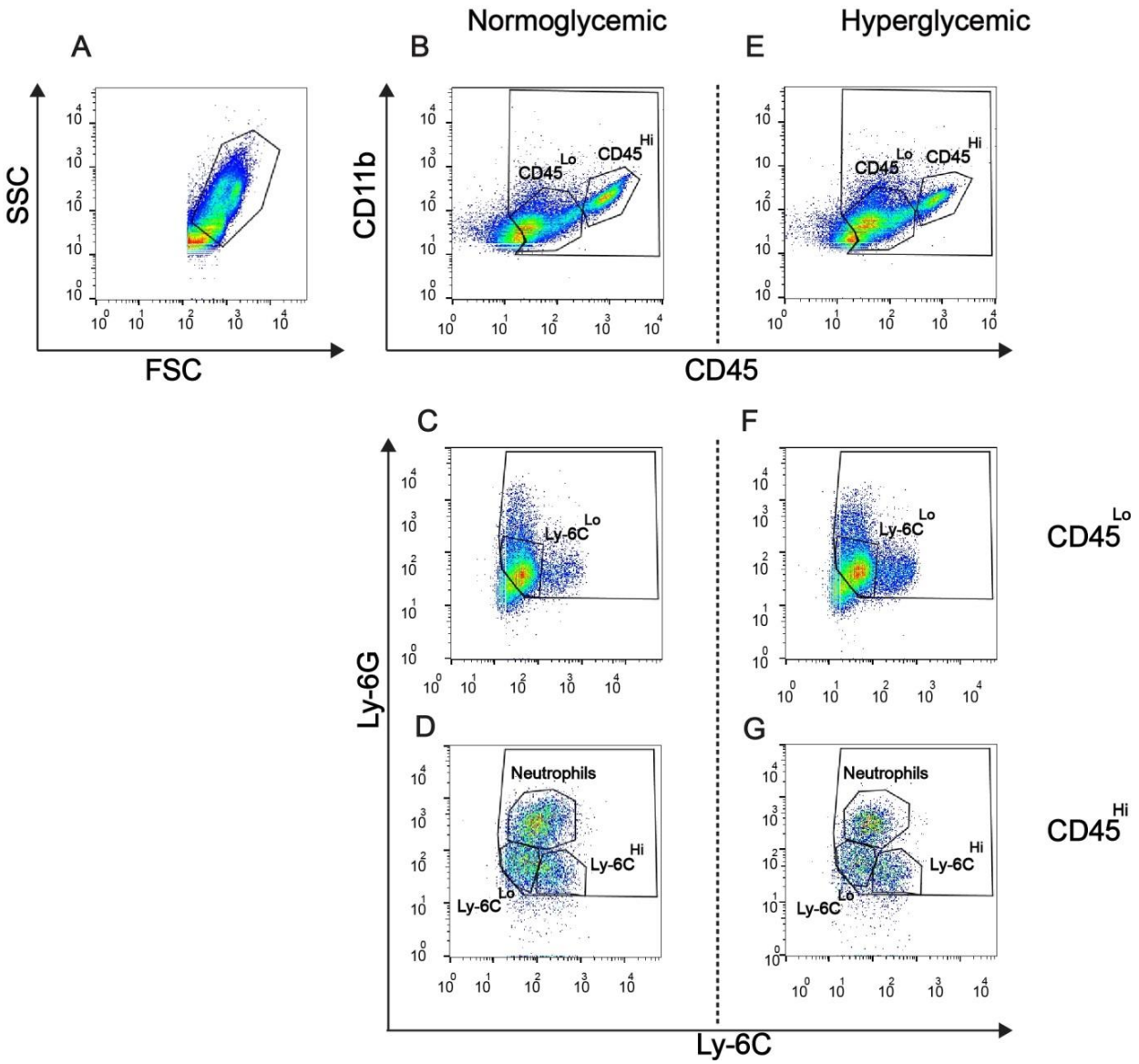

Flow cytometric characterization of ischemic brain under normoglycemic and hyperglycemic conditions. (A) Dot plot shows forward (FSC) and side scatter (SSC) of cells. (B, C, D) Representative dot plots of normoglycemic groups. (E, F, G) Representative dot plots of hyperglycemic group. CD45^{Lo} gated against Ly-6C and Ly-6. (D) Neutrophils, Ly-6C^{Lo} and Ly-6C^{Hi} sub-populations in gated CD45^{Hi} of normoglycemic mice 48 hours after MCAO.

(G) Neutrophils, Ly-6C^{Lo} and Ly-6C^{Hi} sub-populations in gated CD45^{Hi} of hyperglycemic mice 48 hours after MCAO.

Figure 12 Quantification of flow cytometric results.

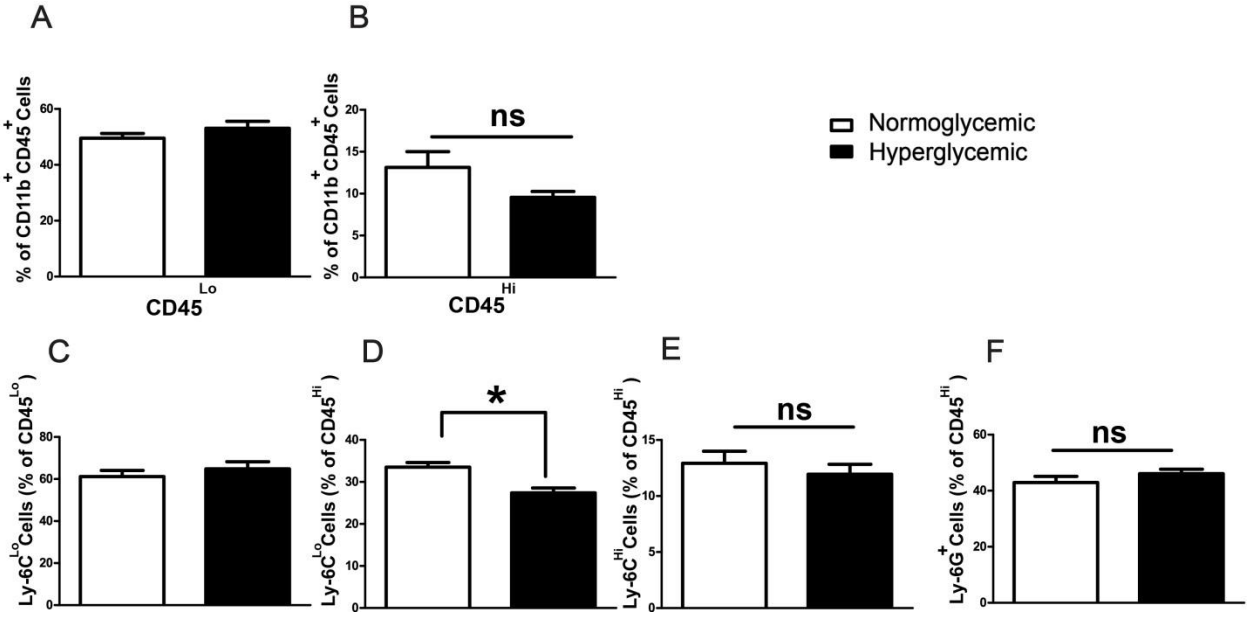

*(A) $CD45^{Lo}$ cells as percentage of total $Cd11b^{+}Cd45^{+}$cells. (B) $CD45^{Hi}$ cells as percentage of total $Cd11b^{+}Cd45^{+}$ cells. (C) Ly-$6C^{Lo}$ cells as percentage of $CD5^{Lo}$ cells. (D) $CD5^{Hi}$ Ly-$6C^{Lo}$ cells as percentage of $CD5^{Hi}$ cells. (E) $CD45^{Hi}$Ly-$6C^{Hi}$ cells as percentage of $CD5^{Hi}$ cells. (F) Ly-$6G^{+}$Ly-$6C^{-}$ neutrophils as percentage of $CD45^{Hi}$ cells. Unpaired t-test, *p<0.03, values are mean ± SEM (n=11/group).*

3.5. Reduced number of arginase I (Arg I) expressing M2 macrophages

In vivo results and flow cytometry results were further confirmed by using immune fluorescence microscopy techniques. A staining technique was established to identify the infiltrating monocytes/macrophages. Arginase I is an important enzyme involved in the degradation of the amino acid toxic product (arginine) to non-toxic one (ornithine). Arginase I expression is induced in BMDC by Th2 cells, when BMDC are incubated with Th2 cells for 48 hours (Munder, Eichmann et al. 1999). In this experiment, MCAO was performed in C57BL/6 mice, under hyperglycemic and normoglycemic conditions. Forty-eight hours after MCAO surgery, the mice were perfused and arginase I staining was performed. The imaging of stained slides was performed with a fluorescence or a confocal microscope. Three regions of interests (ROI) were defined on the periphery of the infarct. The double and single positive cells were counted by using Fiji (NIH free software). The colocalization of Iba1 and arginase I was confirmed by confocal imaging (Figure 13). The double positive arginase I and Iba1 cells were considered to be M2 monocytes/macrophages corresponding to Ly-6C^{Lo} cells, while single Iba1 positive cells were considered as M1 macrophages corresponding to Ly-6C^{Hi} cells. The immunefluorescence microscopy also confirmed the reduced number of M2 macrophages in ischemic brains under hyperglycemic conditions (Figure 13).

Figure 13 Hyperglycemia reduced arginase I positive M2 macrophages.

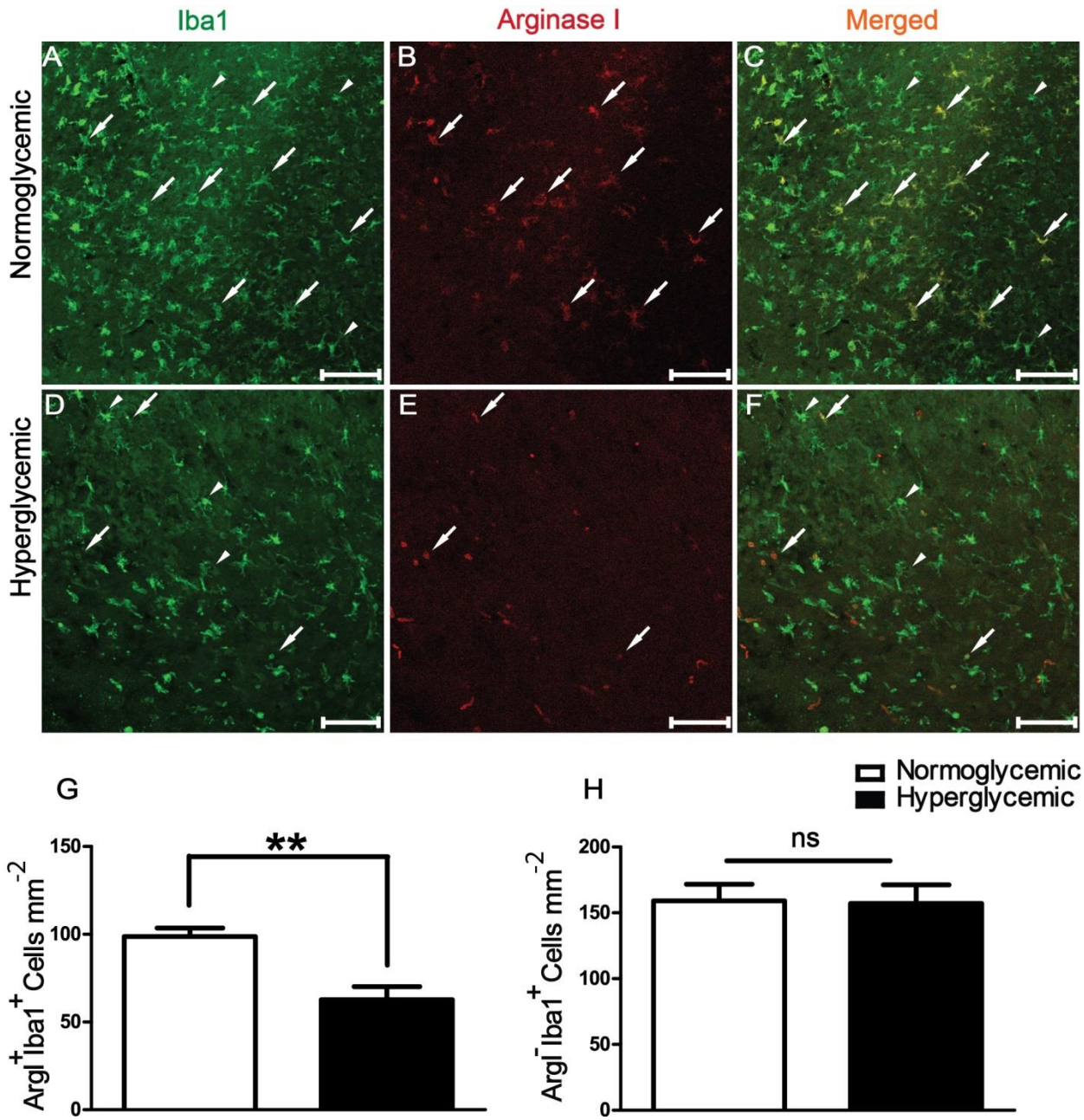

The number of arginase I and Iba1 double positive M2 macrophages is reduced in hyperglycemic mice 48 hours after MCAO. (A-C) Representative confocal images of Iba1 (green) and arginase I (red) staining in normoglycemic group. (D-F) Representative confocal

*images of Iba1 (green) and arginase I (red) staining in the hyperglycemic group. White arrows correspond to M2 monocytes/macrophages and white arrow-heads show M1 monocytes/macrophages. (G-H) Quantification of immune fluorescence microscopy results. Unpaired t-test, **p<0.003, values are mean ± SEM. Scale bar, 100 µm (n=3-4/group).*

3.6. Identifying the role of monocytes/macrophages in hyperglycemic stroke

In different models of inflammation, macrophages perform inflammatory or anti-inflammatory roles (Duffield, Forbes et al. 2005). To identify the role of monocytes/macrophages in brain after induction of stroke, CD11b-DTR mice (n=4 in each group) were utilized, in which monocytes/macrophages can be selectively ablated after administration of diphtheria toxin. Diphtheria toxin was administered i.p (25 ng/g body weight) to both CD11b-DTR mice and their littermate controls. Administration of diphtheria toxin 24 hours and 48 hours before analysis ablated blood monocytes/macrophages. The ablation was confirmed by flow cytometry of blood cells (Figure 14). No significant differences were observed in the accumulation of $CD45^{+}Cd11b^{+}Ly\text{-}6G^{+}Ly\text{-}6C^{-}$ (neutrophils) (Figure 14 M). In contrast, $Cd45^{+}Cd11b^{+}Ly\text{-}6C^{+}Ly\text{-}6G^{-}$ (monocyte/macrophages) were significantly ablated (>80%) in CD11b-DTR mice treated with diphtheria toxin, while the number of these cells remained unaffected in wild-type controls or NaCl treated CD11b-DTR mice (Figure 14 K and L).

Figure 14 ***Diphtheria toxin administration to wild-type controls and CD11b-DTR mice.***

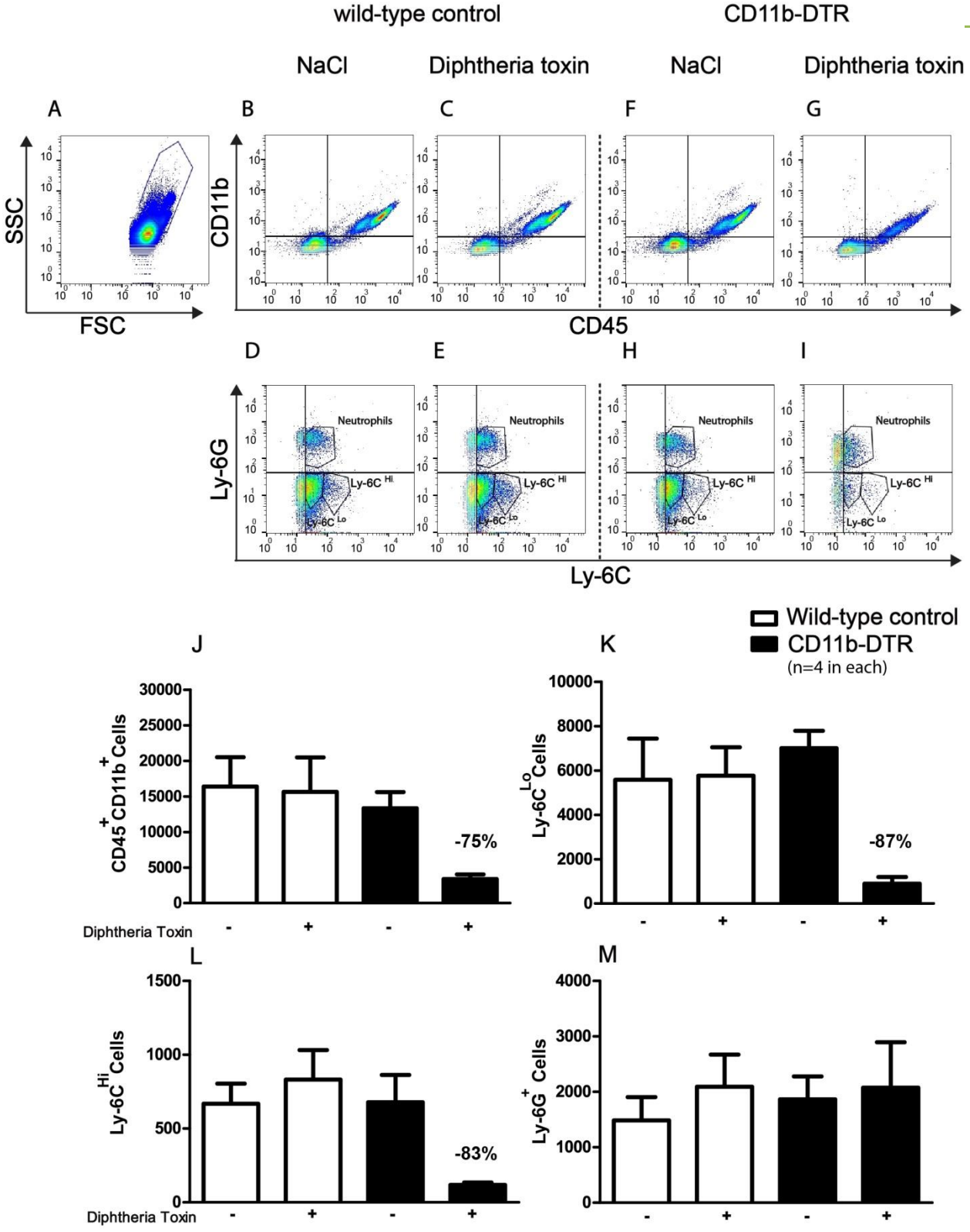

Diphtheria toxin administration to wild-type controls and CD11b-DTR mice (A) Forward and side scatter dot plots of the blood-cells. (B-G) Representative dot plots showing blood cells gated against CD45 and CD11b. Upper right quadrant contains the $CD45^{+}CD11b^{+}$ *population of all groups. (D-I) The* $CD45^{+}CD11b^{+}$ *population gated against Ly-6C and Ly-6G to separate neutrophils,* $Ly\text{-}6C^{Hi}$ *and* $Ly\text{-}6C^{Lo}$ *monocytes/macrophages. (J-M) Quantification of flow cytometry results* (n=10/group). *A 100 µl of whole blood was used to count the cells.*

3.7. Measurement of infarct volume in CD11b-DTR

To identify the effect of monocytes/macrophages depletion on infarct volume, MCAO was performed in CD-11b-DTR mice. Age- and gender-matched mice were randomly divided into normoglycemic (NG) and hyperglycemic (HG) groups. All the mice were treated with diphtheria toxin (25 ng/g body weight). Forty-eight hours after MCAO infarct volume was measured. The results showed that the detrimental effect of hyperglycemia was lost in diphtheria toxin treated CD11b-DTR mice (Figure 15), nevertheless the infarct size in wild-type mice was bigger in hyperglycemic mice than that of normoglycemic mice (Figure 15).

Figure 15 Infarct volume measurements in CD11b-DTR and WT mice.

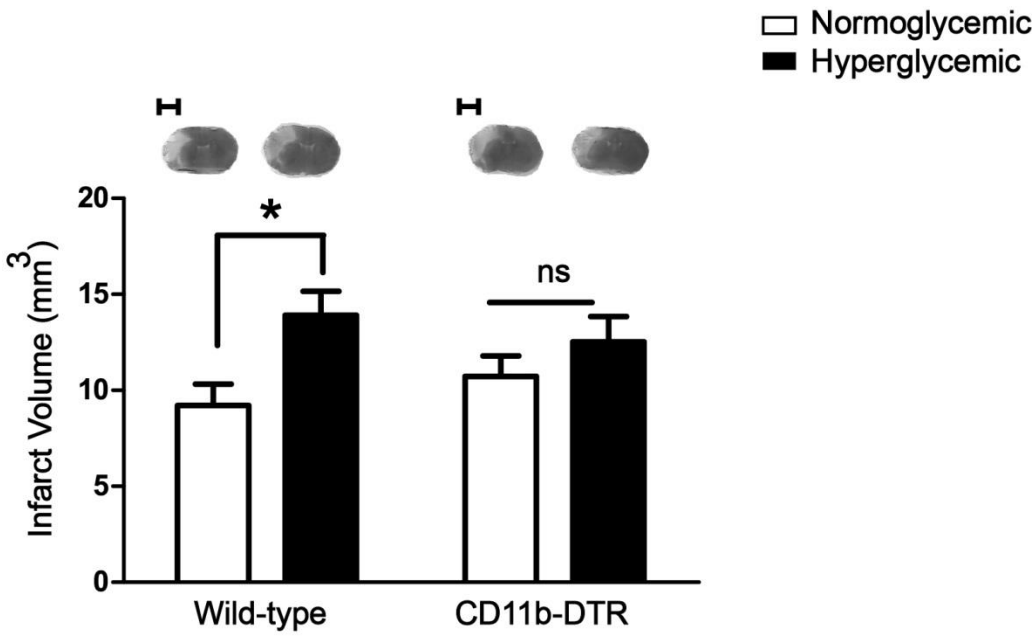

*The detrimental effect of hyperglycemia was lost when CD11b$^+$cells had been ablated. To ablate CD11b$^+$cells, we treated CD11b-DTR mice and wild-type mice with diphtheria toxin. The infarct volume was determined 48 hours after MCAO. Two-way ANOVA, *P<0.05 (Bonferroni posttests). Values are means ± S.E.M. (n=11/group). Scale bar, 2.5 mm.*

3.8. Measurement of infarct volume in RAGE$^{-/-}$

To identify the involvement of RAGE in hyperglycemic stroke we sought to perform an MCAO experiment in RAGE$^{-/-}$ mice. We used 8-10 weeks old RAGE$^{-/-}$ mice and performed MCAO under normoglycemic and hyperglycemic conditions. Forty-eight hours after MCAO, mice were perfused and brains were harvested. Infarct volume measurement showed that hyperglycemic wild-type mice had significantly bigger infarcts than animals in the normoglycemic and hyperglycemic RAGE$^{-/-}$group (Figure 16). Therefore, RAGE mediates the detrimental effect of hyperglycemia in focal cerebral ischemia.

Figure 16 RAGE $^{-/-}$ mice have reduced infarcts compared to wild-type mice during hyperglycemia.

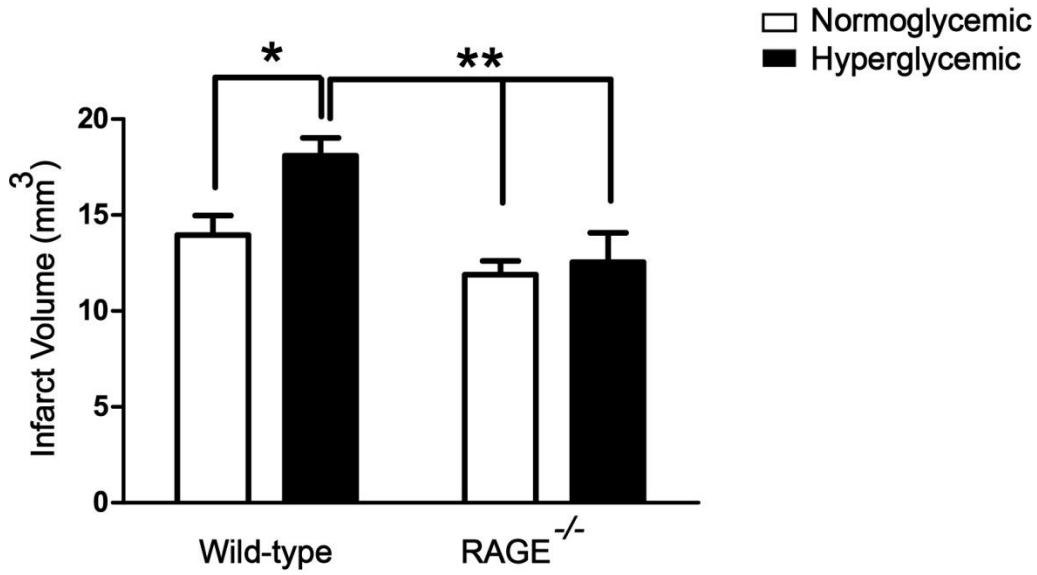

*RAGE $^{-/-}$ mice have reduced infarcts compared with hyperglycemic wild-type mice 48 hours after MCAO. Two-way ANOVA, *P<0.05 (Bonferroni posttests). Values are means ± S.E.M. (n=9/group).*

4. DISCUSSION

4.1. Rodent stroke models

Different rodent models of cerebral ischemia have been used to study the pathophysiology of stroke. The focal (stroke) and global (cardiac arrest) model represent major types of cerebral ischemia. Focal cerebral ischemia is further divided into transient and permanent stroke models (Sicard and Fisher 2009). The choice of a suitable stroke model plays an important role to validate the findings of a preclinical research. In this study, we used a permanent stroke model in mice. In this model, we occluded the distal middle cerebral artery (MCA) permanently. The permanent stroke results in a region of severe damage (ischemic core) which is surrounded by a region of less damage (penumbra). The core is a region which is unable to resist stroke conditions, and the region near the periphery of the infarct is called as penumbra (Bandera, Botteri et al. 2006). The permanent stroke model is advantageous, for example, because of high reproducibility and low mortality rate. The consequence of cerebral ischemia is to reduce the access of oxygen and glucose to the brain tissue. This decline in the supply of essential nutrients to the brain increases the brain damage after ischemia (Traystman 2003). This shows that glucose and oxygen are essential for the integrity of the brain. On the other hand, excess of glucose (hyperglycemia) causes more damage to the ischemic brain instead of being useful. To understand the glucose paradox, this study was conducted.

4.2. Hyperglycemic stroke

Hyperglycemia is considered to be an independent risk factor for stroke (Jorgensen, Nakayama et al. 1994; Wannamethee, Perry et al. 1999; Ahmed, Davalos et al. 2010; Fang, Zhang et al. 2013). Hyperglycemia worsens the stroke outcome by different mechanisms that include reduced blood flow to penumbra (Dandona, James et al. 1978; Duckrow, Beard et al. 1985; Kawai, Keep et al. 1998) modifications in brain metabolism (Folbergrova, Memezawa et al. 1992) increased edema (Berger and Hakim 1986) and most significantly glucose facilitated oxidative stress (Mohanty, Hamouda et al. 2000). In animal stroke models, it has been indicated that rising glucose levels to 10, 15 or 20 mmol/L have an effect in increasing the infarct volume and apoptosis after stroke (Rizk, Rafols et al. 2006; Won, Tang et al. 2011). In vitro data have also shown that 12-15 mmol/L glucose is sufficient to provide hyperglycemic conditions during cell-culture (Krankel, Adams et al. 2005). In our study, a single intraperitoneal injection of 25% glucose (200 µl) before MCAO was able to induce acute hyperglycemia in mice. In humans due to a generalized stress response after stroke, the HPA axis is stimulated that increases the glucose production by different mechanism (Kruyt, Biessels et al. 2010) and ultimately the stroke patients are hyperglycemic (Ziegler and Herman 2002; Kruyt, Biessels et al. 2010). This is why we administered glucose immediately before MCAO to induce acute hyperglycemia. Thirty minutes and 50 minutes after the glucose injection, the blood glucose levels were found to be elevated up to ± 260 mg/dl (14.66 mmol/L) in hyperglycemic mice. These conditions correspond to a clinical situation, in which admission hyperglycemia is observed in stroke patients (Ahmed, Davalos et al. 2010). Forty-eight hours after MCAO, the infarct volume was measured, and it was significantly larger in HG groups than that in NG counterparts. Our results suggest that higher

plasma levels of glucose at the time of ischemia play a crucial role in increasing the infarct size. These data are also consistent with previous findings (Yip, He et al. 1991). In the ischemic brain, there is a region which has very low blood supply after ischemia but still enough to maintain its metabolic functions. This region is called penumbra. Hyperglycemia increases the risk of damage to the penumbra because of increased lactic acid production and damage to the blood-brain barrier (Parsons, Barber et al. 2002).

According to the European stroke organization (ESO) 2008 guideline under the section of good clinical practice (GCP), it is recommended to lower high blood glucose (>180 mg/dl or 10 mM) with insulin titrations and in case of hypoglycemia (<50 mg/dl or 2.8 mM) to treat with i.v dextrose or 10-20% glucose infusion (Anonymous 2008).

4.3. Role of infiltrating immune cells after cerebral ischemia

Blood leukocytes and microglia are activated after the stroke, and these cells migrate to the brain tissue subsequently leading to brain injury (Wang, Tang et al. 2007). After microglial activation, there is a release of different chemokines that attract blood-derived leukocytes to the site of inflammation. Monocyte chemoattractant protein 1 (CCL2/MCP-1) is one of those chemokines that attracts monocytes-derived cells (Hinojosa, Garcia-Bueno et al. 2011). It has been shown previously that infiltration of immature Ly-6C^{Hi} monocytes (M1-macrophages) and their polarization into mature Ly-6C^{Lo} (M2-macrophages) starts as early as 24 hours after MCAO (Gliem, Mausberg et al. 2012).

Macrophages are found at the sites of brain injury where they stimulate both injury and repair. Therefore, the involvement of M1/M2 macrophages cannot be ignored (Kigerl, Gensel et al. 2009). It has also been reported that intense infiltration of immune cells in the brain occurs quiet early after stroke and this infiltration of cells is more pronounced in the absence of reperfusion (Chu, Kim et al. 2014). Previously, we have shown that the ß-hydroxy butyrate (BHB) receptor HCA_2 (GPR109) activates a neuroprotective subset of macrophages. We used Hca2$^{-/-}$, HCA2^{mRFP} and wild-type mice. BHB administration reduced the infarct volume in wild-type mice, but the protective effect was lost in Hca2$^{-/-}$ mice. In parallel, BHB treatment improved to sensory-motor function as shown by the corner test. Nicotinic acid is an agonist of the HCA_2 receptor. The nicotinic acid treatment also reduced infarct volume and neurological outcome after MCAO. To identify the location of HCA_2 receptor, we generated chimeric mice. In those mice, wild-type bone-marrow was transplanted to HCA2^{mRF} (WT > HCA2^{mRF}) and HCA2^{mRF} bone-marrow was transplanted to wild-type mice (HCA2^{mRFP} > WT). Immunofluorescence microscopy confirmed that the HCA_2 receptor is located on bone-marrow derived monocytes/macrophages infiltrating

the brain. Flow cytometry showed that these cells are Ly-6C^{Lo} monocytes/macrophages. The analysis of *mRFP*$^{+}$ cells, in the brain, was performed 24 hours and 48 hours after MCAO.

4.4. Hyperglycemia downregulates M2 macrophages

Keeping in view the role of immune cells in general, and M2 macrophages in particular, we intended to investigate infiltrating immune cells in the brain after MCAO under normoglycemic and hyperglycemic conditions. Forty-eight hours after MCAO mice were perfused with Ringer's lactate and brain cells preparation was done. The brain cells were stained with antibodies against CD45, CD-11b, Ly-6C and Ly-6G. Flow cytometry was used to distinguish different cell-populations. These data have proved that under hyperglycemic conditions, CD45^{Hi}Ly-6C^{Lo}cells (M2 macrophages) are reduced while the number of CD45^{Lo}, CD45^{Hi}, Ly-6C^{Hi} and neutrophils remained unchanged.

4.5. Hyperglycemia reduces arginase I expressing M2-macrophages

Arginases are the group of enzymes involved in the breakdown of arginine to ornithine and urea. Two isoforms of arginase were found, one in cytosolic fractions (Arginase I, Liver arginase) and the other in mitochondrial fractions (Arginase II, kidney arginase) (Jackson, Beaudet et al. 1986). It has been reported that in mouse embryonic development arginases are required and arginase I is the most important form needed (Yu, Iyer et al. 2002). An imbalance in the expression of arginase I isoform, may also cause endothelial dysfunction in the chronic intermittent hypoxia (CIH) rats (Krause, Del Rio et al. 2015). It has been reported that the macrophage-specific expression of arginase I is anti-inflammatory and promotes tissue repair after injury (Pesce, Ramalingam et al. 2009). Arginase I is also specifically expressed by M2 macrophages in the spinal cord after a spinal cord injury (SCI) (Pomeshchik, Kidin et al. 2015). Many other diseases

also confirmed the involvement of arginases (Sindrilaru, Peters et al. 2011; Munro, Perreau et al. 2012; Hochstedler, Leidinger et al. 2013; Turtzo, Lescher et al. 2014). To see a potential effect of hyperglycemia on arginase I expressing cells after stroke, we used Iba1 and arginase I staining on brain sections. Forty-eight hours after MCAO the mice were perfused with Ringer's lactate followed by PFA perfusion and post-fixation. We found macrophagic and microglial responses with features of mixed populations of M1 and M2 phenotypes. Arginase I and Iba1 staining confirmed that the double-positive cells are M2 monocytes/macrophages, while the single Iba1 positive cells were considered as M1 macrophages. Quantitative analysis has shown that after MCAO, the number of arginase I expressing cells is reduced under hyperglycemic conditions in comparison to normoglycemic conditions.

4.6. Role of monocytes/macrophages in hyperglycemic stroke

Conditional ablation of monocytes/macrophages in CD11b-DTR mice is a nice tool to study their role in different diseases. We investigated CD11b-DTR mice and their littermate controls. In these mice, monocytes/macrophages express the human diphtheria toxin receptor under the control of the CD11b promoter (Cailhier, Partolina et al. 2005). The sensitivity of human DTR to diphtheria toxin is 10^3 to 10^5-times higher than mouse DTR. Therefore, when the human DTR is expressed in the mouse, the cells will die in the presence of diphtheria toxin (Chow, Brown et al. 2011). Different studies have confirmed that this technique is used to deplete monocytes/macrophages not only in the peripheral blood but also in different tissues (Cailhier, Sawatzky et al. 2006; Stoneman, Braganza et al. 2007). Therefore using macrophage ablation techniques, throws light on the role of monocytes/macrophages in ischemic stroke under hyperglycemic conditions. We have provided evidence that M2 macrophages are reduced under HG conditions 48 hours after MCAO and these cells are positive for CD11b and Iba1. The Iba1 co-expression showed these cells resemble the morphology of resident macrophages/microglia. After diphtheria toxin administration, there was approximately 80% depletion of blood monocytes/macrophages. The depletion of peripheral monocytes/macrophages was confirmed by flow cytometry of blood cells. Infarct volume measurements showed that hyperglycemic wild-type mice had larger infarcts while this increase in the infarct volume was lost if diphtheria toxin was administered to CD11b-DTR mice. These data confirm the involvement of monocytes/macrophages in controlling the infarct volume under hyperglycemic conditions. These data are also consistent with our previous finding in which nicotinic acid was unable to perform neuroprotective action in the diphtheria toxin treated CD11b-DTR mice, because the HCA_2 receptor for nicotinic acid was found to be located on Ly-$6C^{Lo}$cells.

4.7. RAGE mediates the ischemic brain damage

Our study indicates that RAGE mediates the ischemic brain injury under hyperglycemic conditions. RAGE is a multiligand receptor found on neurons, glia and endothelial cells (Deane, Du Yan et al. 2003). Its role in increasing the brain damage after cerebral ischemia has also been proved (Muhammad, Barakat et al. 2008). The expression of RAGE is increased in the presence of its ligands (Chavakis, Bierhaus et al. 2004). The ligands for RAGE are high mobility box 1 (HMGB1), S100 proteins, amyloid beta peptide (Aß peptide) and several damage-associated molecular pattern molecules (DAMPs) released during tissue damage (Sessa, Gatti et al. 2014). RAGE is expressed by almost all the cells in the brain and its activation leads to formation of reactive oxygen species (ROS). Therefore, an indirect involvement of RAGE in increasing the infarct size is also possible (Yan, Chen et al. 1996; Muhammad, Barakat et al. 2008). In vitro data have reported a hyper-responsive phenotype of human monocytes which produce a burst of superoxide (O_2^-) under hyperglycemic conditions. RAGE is involved in inducing O_2^- generation by its ligand S100B (Ding, Kantarci et al. 2007). The presence of S100B, a RAGE ligand, has been reported in the brain, white fat and testes of diabetic patients (Zimmer, Chessher et al. 1997).

In this study, we have observed significantly reduced infarct volumes in $RAGE^{-/-}$ mice under NG and HG conditions and also the number of M2 monocytes/macrophages is reduced in the hyperglycemic ischemic brains. Therefore, there might be involvement of another phenotype of monocytes that expresses RAGE and increases oxidative stress under hyperglycemic conditions. It can be concluded that in the absence of RAGE, the glycated products are unable to induce cellular disorders or oxidative stress under hyperglycemic conditions

5. CONCLUSION

These data confirm that the M2 monocyte/macrophages are depleted under hyperglycemic conditions and this plays a role in deteriorating the stroke outcome.

6. FUTURE PERSPECTIVE

Considering the hyperglycemic conditions as a predictor of bad stroke outcome, it has been suggested to improve the metabolic conditions by lowering glucose levels. Insulin therapy can be an option (Bruno, Liebeskind et al. 2010; McCormick, Hadley et al. 2010).

AGEs worsen the stroke outcome by interacting with RAGE. Expression of RAGE is upregulated in diabetic patients due to increased levels of its ligands. Therefore, reduction in the level of these compounds can be helpful in reducing the brain damage in stroke patients. Soluble RAGE (sRAGE) is a shortened form of RAGE that inhibits the AGE- mediated signaling by acting as a scavenger (Kankova, Kalousova et al. 2008). Therefore, administration of sRAGE or HMGB1 antagonist would be alternative ways to ameliorate the AGE-RAGE or HMGB1-RAGE mediated brain damage respectively (Muhammad, Barakat et al. 2008).

There is a need for further studies to investigate the mechanism of the involvement of RAGE in mediating the brain damage. The role of the ligands for RAGE (S100A8/S100A9, S100B, and HMGB1) needs to be defined under HG conditions.

The arginase I expression in the ischemic brain is decreased under hyperglycemic conditions and this confirms a lower number of the M2 macrophages. A strategy could be to stimulate the polarization of M2 macrophages. These macrophages would play an important role in reducing hyperglycemic infarcts by promoting the healing process. There is a need for in vitro studies concerning the expression analysis of macrophage colony stimulating factor (MCSF) or CCL2 under hyperglycemic conditions.

Use of antioxidants that may inhibit NF-kB pathway in diabetic patients might be helpful in reducing the inflammation (Hofmann, Schiekofer et al. 1999).

7. REFERENCES

"Hilfsmittel zur Fallzahlplanung." Retrieved 01.01.2012, 2012, from http://www.uni-heidelberg.de/md/tier-schutz/tierschutz/info_planungshilfe.pdf.

Ahmad, M., S. Saleem, et al. (2010). "The PGE2 EP2 receptor and its selective activation are beneficial against ischemic stroke." Exp Transl Stroke Med **2**(1): 12.

Ahmad, M., S. Saleem, et al. (2006). "1-hydroxyPGE reduces infarction volume in mouse transient cerebral ischemia." Eur J Neurosci **23**(1): 35-42.

Ahmed, N., A. Davalos, et al. (2010). "Association of admission blood glucose and outcome in patients treated with intravenous thrombolysis: results from the Safe Implementation of Treatments in Stroke International Stroke Thrombolysis Register (SITS-ISTR)." Arch Neurol **67**(9): 1123-1130.

Allport, L. E., K. S. Butcher, et al. (2004). "Insular cortical ischemia is independently associated with acute stress hyperglycemia." Stroke **35**(8): 1886-1891.

Anderson, R. E., W. K. Tan, et al. (1999). "Effects of glucose and PaO2 modulation on cortical intracellular acidosis, NADH redox state, and infarction in the ischemic penumbra." Stroke **30**(1): 160-170.

Anonymous (2008). "Guidelines for management of ischaemic stroke and transient ischaemic attack 2008." Cerebrovasc Dis **25**(5): 457-507.

Auffray, C., M. H. Sieweke, et al. (2009). "Blood monocytes: development, heterogeneity, and relationship with dendritic cells." Annu Rev Immunol **27**: 669-692.

Bandera, E., M. Botteri, et al. (2006). "Cerebral blood flow threshold of ischemic penumbra and infarct core in acute ischemic stroke: a systematic review." Stroke **37**(5): 1334-1339.

Bargiotas, P., S. Muhammad, et al. (2012). "Connexin 36 promotes cortical spreading depolarization and ischemic brain damage." Brain Res **1479**: 80-85.

Beretta, S., M. Riva, et al. (2013). "Optimized system for cerebral perfusion monitoring in the rat stroke model of intraluminal middle cerebral artery occlusion." J Vis Exp(72).

Berger, L. and A. M. Hakim (1986). "The association of hyperglycemia with cerebral edema in stroke." Stroke **17**(5): 865-871.

Broughton, B. R., D. C. Reutens, et al. (2009). "Apoptotic mechanisms after cerebral ischemia." Stroke **40**(5): e331-339.

Brownlee, M. (1995). "Advanced protein glycosylation in diabetes and aging." Annu Rev Med **46**: 223-234.

Bruno, A., D. Liebeskind, et al. (2010). "Diabetes mellitus, acute hyperglycemia, and ischemic stroke." Curr Treat Options Neurol **12**(6): 492-503.

Cailhier, J. F., M. Partolina, et al. (2005). "Conditional macrophage ablation demonstrates that resident macrophages initiate acute peritoneal inflammation." J Immunol **174**(4): 2336-2342.

Cailhier, J. F., D. A. Sawatzky, et al. (2006). "Resident pleural macrophages are key orchestrators of neutrophil recruitment in pleural inflammation." Am J Respir Crit Care Med **173**(5): 540-547.

Casals, J. B., N. C. Pieri, et al. (2011). "The use of animal models for stroke research: a review." Comp Med **61**(4): 305-313.

Chavakis, T., A. Bierhaus, et al. (2004). "RAGE (receptor for advanced glycation end products): a central player in the inflammatory response." Microbes Infect **6**(13): 1219-1225.

Chow, A., B. D. Brown, et al. (2011). "Studying the mononuclear phagocyte system in the molecular age." Nat Rev Immunol **11**(11): 788-798.

Chu, H. X., H. A. Kim, et al. (2014). "Immune cell infiltration in malignant middle cerebral artery infarction: comparison with transient cerebral ischemia." J Cereb Blood Flow Metab **34**(3): 450-459.

Counsell, C., M. McDowall, et al. (1997). "Hyperglycaemia after acute stroke. Other models find that hyperglycaemia is not independent predictor." BMJ **315**(7111): 810; author reply 811.

Dal-Secco, D., J. Wang, et al. (2015). "A dynamic spectrum of monocytes arising from the in situ reprogramming of CCR2+ monocytes at a site of sterile injury." J Exp Med **212**(4): 447-456.

Dandona, P., I. M. James, et al. (1978). "Cerebral blood flow in diabetes mellitus: evidence of abnormal cerebrovascular reactivity." Br Med J **2**(6133): 325-326.

Davis, M. F., C. Lay, et al. (2013). "Permanent cerebral vessel occlusion via double ligature and transection." J Vis Exp(77).

Deane, R., S. Du Yan, et al. (2003). "RAGE mediates amyloid-beta peptide transport across the blood-brain barrier and accumulation in brain." Nat Med **9**(7): 907-913.

Dietrich, W. D., M. D. Ginsberg, et al. (1986). "Photochemically induced cortical infarction in the rat. 2. Acute and subacute alterations in local glucose utilization." J Cereb Blood Flow Metab **6**(2): 195-202.

Ding, Y., A. Kantarci, et al. (2007). "Activation of RAGE induces elevated O2- generation by mononuclear phagocytes in diabetes." J Leukoc Biol **81**(2): 520-527.

Dirnagl, U., C. Iadecola, et al. (1999). "Pathobiology of ischaemic stroke: an integrated view." Trends Neurosci **22**(9): 391-397.

Duckrow, R. B., D. C. Beard, et al. (1985). "Regional cerebral blood flow decreases during hyperglycemia." Ann Neurol **17**(3): 267-272.

Duffield, J. S., S. J. Forbes, et al. (2005). "Selective depletion of macrophages reveals distinct, opposing roles during liver injury and repair." J Clin Invest **115**(1): 56-65.

Fang, Y., S. Zhang, et al. (2013). "Hyperglycaemia in acute lacunar stroke: a Chinese hospital-based study." Diab Vasc Dis Res **10**(3): 216-221.

Folbergrova, J., H. Memezawa, et al. (1992). "Focal and perifocal changes in tissue energy state during middle cerebral artery occlusion in normo- and hyperglycemic rats." J Cereb Blood Flow Metab **12**(1): 25-33.

Galli, S. J., N. Borregaard, et al. (2011). "Phenotypic and functional plasticity of cells of innate immunity: macrophages, mast cells and neutrophils." Nat Immunol **12**(11): 1035-1044.

Garg, R., A. Chaudhuri, et al. (2006). "Hyperglycemia, insulin, and acute ischemic stroke: a mechanistic justification for a trial of insulin infusion therapy." Stroke **37**(1): 267-273.

Gliem, M., A. K. Mausberg, et al. (2012). "Macrophages prevent hemorrhagic infarct transformation in murine stroke models." Ann Neurol **71**(6): 743-752.

Goldin, A., J. A. Beckman, et al. (2006). "Advanced glycation end products: sparking the development of diabetic vascular injury." Circulation **114**(6): 597-605.

Gordon, S. and P. R. Taylor (2005). "Monocyte and macrophage heterogeneity." Nat Rev Immunol **5**(12): 953-964.

Hanson, J., A. Gille, et al. (2010). "Nicotinic acid- and monomethyl fumarate-induced flushing involves GPR109A expressed by keratinocytes and COX-2-dependent prostanoid formation in mice." J Clin Invest **120**(8): 2910-2919.

Hinojosa, A. E., B. Garcia-Bueno, et al. (2011). "CCL2/MCP-1 modulation of microglial activation and proliferation." J Neuroinflammation **8**: 77.

Hochstedler, C. M., M. R. Leidinger, et al. (2013). "Immunohistochemical detection of arginase-I expression in formalin-fixed lung and other tissues." J Histotechnol **36**(4): 128-134.

Hofmann, M. A., S. Schiekofer, et al. (1999). "Peripheral blood mononuclear cells isolated from patients with diabetic nephropathy show increased activation of the oxidative-stress sensitive transcription factor NF-kappaB." Diabetologia **42**(2): 222-232.

Iadecola, C. and J. Anrather (2011). "The immunology of stroke: from mechanisms to translation." Nat Med **17**(7): 796-808.

Ingersoll, M. A., A. M. Platt, et al. (2011). "Monocyte trafficking in acute and chronic inflammation." Trends Immunol **32**(10): 470-477.

Jackson, M. J., A. L. Beaudet, et al. (1986). "Mammalian urea cycle enzymes." Annu Rev Genet **20**: 431-464.

Jin, R., G. Yang, et al. (2010). "Inflammatory mechanisms in ischemic stroke: role of inflammatory cells." J Leukoc Biol **87**(5): 779-789.

Jorgensen, H., H. Nakayama, et al. (1994). "Stroke in patients with diabetes. The Copenhagen Stroke Study." Stroke **25**(10): 1977-1984.

Kankova, K., M. Kalousova, et al. (2008). "Soluble RAGE, diabetic nephropathy and genetic variability in the AGER gene." Arch Physiol Biochem **114**(2): 111-119.

Kawai, N., R. F. Keep, et al. (1998). "Hyperglycemia induces progressive changes in the cerebral microvasculature and blood-brain barrier transport during focal cerebral ischemia." Acta Neurochir Suppl **71**: 219-221.

Kiefer, A. S., T. Fleming, et al. (2014). "Methylglyoxal concentrations differ in standard and washed neonatal packed red blood cells." Pediatr Res **75**(3): 409-414.

Kigerl, K. A., J. C. Gensel, et al. (2009). "Identification of two distinct macrophage subsets with divergent effects causing either neurotoxicity or regeneration in the injured mouse spinal cord." J Neurosci **29**(43): 13435-13444.

Kirby, A., V. Gebski, et al. (2002). "Determining the sample size in a clinical trial." Med J Aust **177**(5): 256-257.

Kissela, B. M., J. Khoury, et al. (2005). "Epidemiology of ischemic stroke in patients with diabetes: the greater Cincinnati/Northern Kentucky Stroke Study." Diabetes Care **28**(2): 355-359.

Krankel, N., V. Adams, et al. (2005). "Hyperglycemia reduces survival and impairs function of circulating blood-derived progenitor cells." Arterioscler Thromb Vasc Biol **25**(4): 698-703.

Krause, B. J., R. Del Rio, et al. (2015). "Arginase-endothelial nitric oxide synthase imbalance contributes to endothelial dysfunction during chronic intermittent hypoxia." J Hypertens **33**(3): 515-524.

Kruyt, N. D., G. J. Biessels, et al. (2010). "Hyperglycemia in acute ischemic stroke: pathophysiology and clinical management." Nat Rev Neurol **6**(3): 145-155.

Matz, K., K. Keresztes, et al. (2006). "Disorders of glucose metabolism in acute stroke patients: an underrecognized problem." Diabetes Care **29**(4): 792-797.

McCormick, M., D. Hadley, et al. (2010). "Randomized, controlled trial of insulin for acute poststroke hyperglycemia." Ann Neurol **67**(5): 570-578.

McTigue, D. M., M. Tani, et al. (1998). "Selective chemokine mRNA accumulation in the rat spinal cord after contusion injury." J Neurosci Res **53**(3): 368-376.

Mecca, A. P., R. W. Regenhardt, et al. (2011). "Cerebroprotection by angiotensin-(1-7) in endothelin-1-induced ischaemic stroke." Exp Physiol **96**(10): 1084-1096.

Mohanty, P., W. Hamouda, et al. (2000). "Glucose challenge stimulates reactive oxygen species (ROS) generation by leucocytes." J Clin Endocrinol Metab **85**(8): 2970-2973.

Mosser, D. M. and J. P. Edwards (2008). "Exploring the full spectrum of macrophage activation." Nat Rev Immunol **8**(12): 958-969.

Moulin, T., L. Tatu, et al. (1997). "The Besancon Stroke Registry: an acute stroke registry of 2,500 consecutive patients." Eur Neurol **38**(1): 10-20.

Muhammad, S., W. Barakat, et al. (2008). "The HMGB1 receptor RAGE mediates ischemic brain damage." J Neurosci **28**(46): 12023-12031.

Munder, M., K. Eichmann, et al. (1999). "Th1/Th2-regulated expression of arginase isoforms in murine macrophages and dendritic cells." J Immunol **163**(7): 3771-3777.

Munro, K. M., V. M. Perreau, et al. (2012). "Differential gene expression in the EphA4 knockout spinal cord and analysis of the inflammatory response following spinal cord injury." PLoS One **7**(5): e37635.

Murray, P. J. and T. A. Wynn (2011). "Protective and pathogenic functions of macrophage subsets." Nat Rev Immunol **11**(11): 723-737.

Okouchi, M., O. Ekshyyan, et al. (2007). "Neuronal apoptosis in neurodegeneration." Antioxid Redox Signal **9**(8): 1059-1096.

Parsons, M. W., P. A. Barber, et al. (2002). "Acute hyperglycemia adversely affects stroke outcome: a magnetic resonance imaging and spectroscopy study." Ann Neurol **52**(1): 20-28.

Passlick, B., D. Flieger, et al. (1989). "Identification and characterization of a novel monocyte subpopulation in human peripheral blood." Blood **74**(7): 2527-2534.

Pesce, J. T., T. R. Ramalingam, et al. (2009). "Arginase-1-expressing macrophages suppress Th2 cytokine-driven inflammation and fibrosis." PLoS Pathog **5**(4): e1000371.

Pomeshchik, Y., I. Kidin, et al. (2015). "Interleukin-33 treatment reduces secondary injury and improves functional recovery after contusion spinal cord injury." Brain Behav Immun **44**: 68-81.

Rahman, M., S. Muhammad, et al. (2014). "The β-hydroxybutyrate receptor HCA2 activates a neuroprotective subset of macrophages." Nat Commun **5**.

Rizk, N. N., J. A. Rafols, et al. (2006). "Cerebral ischemia-induced apoptosis and necrosis in normal and diabetic rats: effects of insulin and C-peptide." Brain Res **1096**(1): 204-212.

Robbins, N. M. and R. A. Swanson (2014). "Opposing effects of glucose on stroke and reperfusion injury: acidosis, oxidative stress, and energy metabolism." Stroke **45**(6): 1881-1886.

Robert K. Murray, D. K. G., Peter A. Mayes, Victor W. Rodwell (2003). Harper's Illustrated Biochemistry, Lange Medical Books/McGraw-Hill, Medical Publishing Division.

Rogers, I. T., D. J. Holder, et al. (1999). "Influence of Blood Collection Sites on Plasma Glucose and Insulin Concentration in Conscious C57BL/6 Mice." Contemp Top Lab Anim Sci **38**(6): 25-28.

Serbina, N. V., T. Jia, et al. (2008). "Monocyte-mediated defense against microbial pathogens." Annu Rev Immunol **26**: 421-452.

Sessa, L., E. Gatti, et al. (2014). "The receptor for advanced glycation end-products (RAGE) is only present in mammals, and belongs to a family of cell adhesion molecules (CAMs)." PLoS One **9**(1): e86903.

Shmonin, A., E. Melnikova, et al. (2014). "Characteristics of cerebral ischemia in major rat stroke models of middle cerebral artery ligation through craniectomy." Int J Stroke **9**(6): 793-801.

Sicard, K. M. and M. Fisher (2009). "Animal models of focal brain ischemia." Exp Transl Stroke Med **1**: 7.

Siesjo, B. K. (1978). "Brain energy metabolism and catecholaminergic activity in hypoxia, hypercapnia and ischemia." J Neural Transm Suppl(14): 17-22.

Sindrilaru, A., T. Peters, et al. (2011). "An unrestrained proinflammatory M1 macrophage population induced by iron impairs wound healing in humans and mice." J Clin Invest **121**(3): 985-997.

Speetzen, L. J., M. Endres, et al. (2013). "Bilateral common carotid artery occlusion as an adequate preconditioning stimulus to induce early ischemic tolerance to focal cerebral ischemia." J Vis Exp(75): e4387.

Spencer, E. A., K. L. Pirie, et al. (2008). "Diabetes and modifiable risk factors for cardiovascular disease: the prospective Million Women Study." Eur J Epidemiol **23**(12): 793-799.

Spite, M. and C. N. Serhan (2010). "Novel lipid mediators promote resolution of acute inflammation: impact of aspirin and statins." Circ Res **107**(10): 1170-1184.

Srikanth, V., A. Maczurek, et al. (2011). "Advanced glycation endproducts and their receptor RAGE in Alzheimer's disease." Neurobiol Aging **32**(5): 763-777.

Stoneman, V., D. Braganza, et al. (2007). "Monocyte/macrophage suppression in CD11b diphtheria toxin receptor transgenic mice differentially affects atherogenesis and established plaques." Circ Res **100**(6): 884-893.

Thornalley, P. J. (2005). "Dicarbonyl intermediates in the maillard reaction." Ann N Y Acad Sci **1043**: 111-117.

Traystman, R. J. (2003). "Animal models of focal and global cerebral ischemia." ILAR J **44**(2): 85-95.

Turtzo, L. C., J. Lescher, et al. (2014). "Macrophagic and microglial responses after focal traumatic brain injury in the female rat." J Neuroinflammation **11**: 82.

Vlassara, H., M. Brownlee, et al. (1981). "Nonenzymatic glycosylation of peripheral nerve protein in diabetes mellitus." Proc Natl Acad Sci U S A **78**(8): 5190-5192.

Wang, Q., X. N. Tang, et al. (2007). "The inflammatory response in stroke." J Neuroimmunol **184**(1-2): 53-68.

Wannamethee, S. G., I. J. Perry, et al. (1999). "Nonfasting serum glucose and insulin concentrations and the risk of stroke." Stroke **30**(9): 1780-1786.

Watson, B. D., W. D. Dietrich, et al. (1985). "Induction of reproducible brain infarction by photochemically initiated thrombosis." Ann Neurol **17**(5): 497-504.

Weir, C. J., G. D. Murray, et al. (1997). "Is hyperglycaemia an independent predictor of poor outcome after acute stroke? Results of a long-term follow up study." BMJ **314**(7090): 1303-1306.

Weiss, J. and F. Zimmermann (1999). "Tribromoethanol (Avertin) as an anaesthetic in mice." Lab Anim **33**(2): 192-193.

Won, S. J., X. N. Tang, et al. (2011). "Hyperglycemia promotes tissue plasminogen activator-induced hemorrhage by Increasing superoxide production." Ann Neurol **70**(4): 583-590.

Yan, S. D., X. Chen, et al. (1996). "RAGE and amyloid-beta peptide neurotoxicity in Alzheimer's disease." Nature **382**(6593): 685-691.

Yip, P. K., Y. Y. He, et al. (1991). "Effect of plasma glucose on infarct size in focal cerebral ischemia-reperfusion." Neurology **41**(6): 899-905.

Yu, H., R. K. Iyer, et al. (2002). "Arginase expression in mouse embryonic development." Mech Dev **115**(1-2): 151-155.

Ziegler, D. R. and J. P. Herman (2002). "Neurocircuitry of stress integration: anatomical pathways regulating the hypothalamo-pituitary-adrenocortical axis of the rat." Integr Comp Biol **42**(3): 541-551.

Zimmer, D. B., J. Chessher, et al. (1997). "S100A1 and S100B expression and target proteins in type I diabetes." Endocrinology **138**(12): 5176-5183.